

الجمهورية الجزائرية الديمقراطية الشعبية

Democratic and Popular Republic of Algeria

وزارة التعليم العالي والبحث العلمي

Ministry of Higher Education and Scientific Research

University of Abbes Laghrour\_ Khenchela

Faculty: Science and Technology

Department: Material sciences



جامعة عباس لغرور خنشلة

كلية العلوم والتكنولوجيا

قسم: علوم المادة

A thesis submitted to obtain the diploma of

Master's Degree (LMD) in Materials Physics

Field: Physics

Specialty: Materials physics

THEME

*Evolution of microstructure and mechanical properties of Ti-N coatings*

**Realized by:**

- *Hassad Ali*
- *Seraoui Merwa*

**Directed by:**

*Dr. Linda Aissani*

**Jury members:**

Dr. Dris Boubaa

Dr. Dounia Adnane

# Acknowledgements

*First and foremost, I would like to thank God for giving us the will and the courage to complete this work.*

*Initially, I give my thank and heartfelt gratitude to my mentor, Dr. Linda Aissani, Who contributed to motivating and guiding us constantly, in addition to benefiting from her valuable scientific skills.*

*I express my sincere appreciation to my reading committee members, Dr. Boubaa Dris and Dr. Adnane Dounia for their precious time to read my work and for accepting to judge it.*

*I would like to extend my special thanks to Dr. Fyza for helping me especially at the beginning of this research.*

*Finally, I would like to acknowledge my heartfelt gratitude to my family and everyone who encouraged me to accomplish this research work.*

# Dedicace

*We dedicate this work to:*

- *To our dear parents, for their continuous support and motivation*
- *To our dear brothers and sisters*
- *All our friends and colleagues*
- *All our relatives and neighbors*

***Ali and Merwa***

# *Contents*

# contents

---

Acknowledgments	
Dedication	
Contents	
List of Figures	
List of tables	
List of symbols	
List of acronyms	
General introduction	1
<hr/>	
<b>Chapter I : Literature Review</b>	
<hr/>	
<b>I.1. Introduction</b>	5
<b>I.2. Thin films</b>	5
<b>I.2.1. Type of thin films</b>	5
<i>I.2.1.1. Monolayer film</i>	6
<i>I.2.1.1. Multilayer film</i>	6
<b>I.3. Deposition technique</b>	6
<b>I.3.1. Physical deposition techniques</b>	8
<b>I.3.1.1. Evaporation techniques</b>	8
<b>I.3.1.1.1. Vacuum thermal Evaporation technique</b>	8
<b>I.3.1.1.2. Electron beam evaporation</b>	8
<b>I.3.1.1.3. Laser beam evaporation (pulsed-laser deposition)</b>	9
<b>I.3.1.2. Sputtering technique</b>	10
<b>I.3.1.2.1. Direct current sputtering</b>	10
<b>I.3.1.2.2. Radio frequency sputtering</b>	11
<b>I.3.2. Chemical Deposition Techniques</b>	12
<b>I.3.2.1. Chemical Vapor Deposition</b>	12
<b>I.3.2.1.1. Low-pressure chemical vapor deposition</b>	13
<b>I.3.2.1.2. Atomic layer deposition</b>	13
<b>I.3.2.2. Chemical Bath Deposition</b>	14
<b>I.3.2.3 Successive Ionic Layer Adsorption and Reaction</b>	15
<b>I.4. Thin film growth modes</b>	15
<b>I.4.1. Island growth mode</b>	16

<b>I.4.2.</b> Layer-by-layer growth mode	17
<b>I.4.3.</b> Layer-by-layer followed by island growth mode	17
<b>I.5.</b> Application of thin films	18
<b>I.6.</b> Titanium	19
<b>I.6.1.</b> Discovery of Titanium	19
<b>I.6.2.</b> Characteristics	19
<b>I.6.3.</b> Crystal Structure	20
<b>I.6.4.</b> Properties of titanium	21
<b>I.6.5.</b> Isotopes of Titanium	23
<b>I.6.6.</b> Titanium Uses	23
<b>I.7.</b> Titanium nitride	23
<b>I.7.1.</b> Structure and properties of titanium nitride	24
<b>I.7.2.</b> Applications	27
<b>I.7.3.</b> Effect of nitrogen content on the properties of TiN thin films	27
<b>I.7.4.</b> Effect of Bias Voltage on the Properties of Ti-N Films	27
<b>I.7.5.</b> Temperature effect on the mechanical and tribological properties of titanium nitride thin films	28
<b>I.8.</b> Conclusion	29
References	30

---

## Chapter II : Experimental techniques

---

<b>II.1.</b> Introduction	35
<b>II.2.</b> X-Ray Diffraction	35
<b>II.2.1.</b> The advantages of XRD	36
<b>II.2.2.</b> The X-Ray diffraction equipment	37
<b>II.2.3.</b> BRAGG'S LAW	37
<b>II.2.3.1</b> Derivation of Bragg's Law	38
<b>II.2.3.2.</b> Applications of Bragg's Law	40
<b>II.3.</b> Microanalyses	40
<b>II.3.1.</b> Energy-Dispersive X-Ray Spectroscopy (EDS)	40
<b>II.3.1.1.</b> Principles of EDS	41
<b>II.3.1.2.</b> EDS analysis applications	41
<b>II.3.2.</b> Wavelength Dispersive Spectroscopy (WDS)	42
<b>II.3.2.1</b> Principles of WDS	42
<b>II.3.2.1.2</b> Applications	43
<b>II.4.</b> Scanning electron microscopy (SEM)	44

<b>II.4.1. SEM Principle</b>	45
<b>II.5. Nanoindentation</b>	46
<b>II.5.1. Definition</b>	46
<b>II.5.2. Nanoindentation Principles</b>	46
<b>II.5.3. Applications of Nanoindentation</b>	47
<b>II.6. Hardness and Young's modulus</b>	47
<b>II.7. Conclusion</b>	51
References	52
<hr/>	
<b>Chapter III: Formation of Titanium Nitrides</b>	
<hr/>	
<b>III.1. Introduction</b>	55
<b>III.2. Experimental details</b>	55
<b>III.3. Results and discussion</b>	56
<b>III.3.1. Chemical composition of TiN coatings</b>	56
<b>III.3.2. Crystalline structure</b>	56
<b>III.3.3. Morphology</b>	58
<b>III. 3. 4. Mechanical property</b>	59
<b>III.4. Conclusion</b>	61
References	62
<hr/>	
General conclusion	65
Abstract	67
<hr/>	

# List of Figures

## *Figures of chapter I*

<b>Figure I.1</b>	<i>Schematic of thin film deposited on a substrate.</i>	<b>5</b>
<b>Figure I.2</b>	<i>The structure coatings (a) monolayer (b) multilayer</i>	<b>6</b>
<b>Figure I.3</b>	<i>Schematic of thermal evaporation system with substrate holder on a planetary rotation system and directly above the evaporating source</i>	<b>8</b>
<b>Figure I.4</b>	<i>Schematic of electron beam evaporation</i>	<b>9</b>
<b>Figure I.5</b>	<i>Schematic of pulsed laser deposition technique</i>	<b>9</b>
<b>Figure I.6</b>	<i>Schematic of the sputtering phenomenon</i>	<b>10</b>
<b>Figure I.7</b>	<i>Schematic diagram of DC sputtering</i>	<b>11</b>
<b>Figure I.8</b>	<i>Schematic diagram of radio frequency planar magnetron</i>	<b>11</b>
<b>Figure I.9</b>	<i>Schematic of general elementary steps of a typical CVD process</i>	<b>12</b>
<b>Figure I.10</b>	<i>LPCVD Process</i>	<b>13</b>
<b>Figure I.11</b>	<i>Atomic layer deposition (ALD)</i>	<b>13</b>
<b>Figure I.12</b>	<i>Experimental set up of CBD technique</i>	<b>14</b>
<b>Figure I.13</b>	<i>Schematic representation of SILAR method</i>	<b>15</b>
<b>Figure I.14</b>	<i>A schematic diagram of thin-film growth steps</i>	<b>16</b>
<b>Figure I.15</b>	<i>Different thin film growth mechanisms</i>	<b>18</b>
<b>Figure I.16</b>	<i>Titanium location in the periodic table</i>	<b>19</b>
<b>Figure I.17</b>	<i>(A) <math>\beta</math> titanium of BCC.,(B) hexagonal unit cell of the <math>\alpha</math> phase</i>	<b>20</b>
<b>Figure I.18</b>	<i>Slip systems</i>	<b>21</b>
<b>Figure I.19</b>	<i>Ti-N Phase Diagrams</i>	<b>24</b>
<b>Figure I.20</b>	<i>Different polymorphic forms of titanium nitride</i>	<b>25</b>

### *Figures of chapter II*

<b>Figure II.1</b>	<b>Principle of X-ray diffraction</b>	<b>35</b>
<b>Figure II.2</b>	<b>Full width at half maximum (FWHM) of an arbitrary peak</b>	<b>36</b>
<b>Figure II.3</b>	<b>Deriving Bragg's Law using the reflection geometry and applying trigonometry</b>	<b>39</b>
<b>Figure II.4</b>	<b>Energy dispersive X-ray spectroscopy</b>	<b>41</b>
<b>Figure II.5</b>	<b>Configuration of sample, analytical crystal and detector on the Rowland circle within the WD spectrometer</b>	<b>43</b>
<b>Figure II.6</b>	<b>SEM micrographs of titanium nitride coatings</b>	<b>44</b>
<b>Figure II.7</b>	<b>Basic components of an SEM</b>	<b>45</b>
<b>Figure II.8</b>	<b>Most common tip geometries and corresponding applications</b>	<b>46</b>
<b>Figure II.9</b>	<b>Schematic of an indentation test</b>	<b>47</b>
<b>Figure II.10</b>	<b>Schematic of the load-displacement curve</b>	<b>49</b>
<b>Figure II.11</b>	<b>Contact geometry parameters</b>	<b>49</b>

### *Figures of chapter III*

<b>Figure III. 1</b>	<b>XRD spectra of the Ti-N coatings deposited at different nitrogen percentage</b>	<b>57</b>
<b>Figure III. 2</b>	<b>SEM cross section and surface images of the TiN coatings deposited at: a) 10 %N<sub>2</sub>, b) 20 %N<sub>2</sub></b>	<b>59</b>
<b>Figure III. 3</b>	<b>Hardness (H) and elastic modulus (E) of the TiN coatings at different N<sub>2</sub>percentage</b>	<b>60</b>

# List of Tables

## *Tables of chapter I*

<b>Tableau I-1</b>	<i>Properties and applications of thin film</i>	<b>18</b>
<b>Tableau I-2</b>	<i>Physical Properties of titanium</i>	<b>21</b>
<b>Tableau I-3</b>	<i>Mechanical Properties of titanium</i>	<b>22</b>
<b>Tableau I-4</b>	<i>Chemical Properties of titanium</i>	<b>22</b>
<b>Tableau I-5</b>	<i>Thermal Properties of titanium</i>	<b>22</b>
<b>Tableau I-6</b>	<i>Phases of TiN</i>	<b>23</b>
<b>Tableau I-7</b>	<i>Properties of Ti and TiN, at Room Temperature</i>	<b>24</b>

## *Tables of chapter III*

<b>Table III. 1</b>	<i>deposition conditions for TiN coatings deposited by R.F magnetron sputtering with different nitrogen percentages</i>	<b>55</b>
<b>Table III. 2</b>	<i>Chemical composition, film thickness, lattice parameter, grain size of the TiN coatings</i>	<b>56</b>

# List of Symbols

<b>Symbol</b>	<b><i>name</i></b>	<b>Unit</b>
<b><math>\lambda</math></b>	<b>wavelength</b>	<b>nm</b>
<b>B</b>	<b>full width half maximum</b>	<b>rad</b>
<b>C</b>	<b>speed of light</b>	<b>m/s</b>
<b><math>\Theta</math></b>	<b><i>Angle between the incident ray and the (hkl) scattering planes.</i></b>	<b>°</b>
<b>H</b>	<b>Max Planck's constant</b>	<b>J.s</b>
<b>P</b>	<b>Pressure</b>	<b>pa</b>
<b>D</b>	<b>The average grain size</b>	<b>nm</b>
<b>H</b>	<b>hardness</b>	<b>Gpa</b>
<b>E</b>	<b>Elastic modulus</b>	<b>Gpa</b>
<b>A</b>	<b>Lattice parameter</b>	<b>nm</b>

# List of acronyms

LPCVD	Low pressure chemical vapor deposition (LPCVD)
PECVD	Plasma-enhanced chemical vapor deposition
ALD	Atomic layer deposition
CVD	Chemical Vapor Deposition
VPE	Vapor-Phase Epitaxy
CBD	Chemical bath deposition
SILAR	Successive ionic layer adsorption and reaction
V-W	Volmer –Weber growth mode
F-M	Frank-van der Merwe growth mode
S-K	Stranski-Krastanov
Ti	Titanium
BCC	body-centered cubic
HCP	hexagonal close-packed
f.c.c	Face-centred-cubic
XRD	X-Ray Diffraction
FWHM	Full Width at Half Maximum
Å	Angstrom unit, $10^{-10}$ m
a, c	Lattice constant; a alone refers to cubic systems.
$\alpha$ , $\beta$	hcp and bcc phases of Ti, respectively.
$\epsilon$	One of the two phases of $Ti_2N$ , 33% at. N.
$\delta'$	One of the two phases of $Ti_2N$ ; -38 at. % N.
$\Delta$	Major nitride phase TiN.
Ev	<i>Electron Volt.</i>
MeV	<i>Mega electron Volt.</i>
KeV	Kilo electron volt
UV	<i>ultraviolet rays</i>

<b>D</b>	<b>spacing between the crystal lattice planes</b>
<b>(XEDS, EDS, or EDX)</b>	<b>Energy-Dispersive X-Ray Spectroscopy</b>
<b>WDS</b>	<b>Wavelength Dispersive Spectroscopy</b>
<b>SEM</b>	<b>Scanning electron microscope</b>
<b>HV</b>	<b>Vickers hardness test (HV)</b>
<b>HK</b>	<b>Knoop hardness test</b>
<b>H</b>	<b>Hardness</b>
<b>E</b>	<b>elastic modulus</b>
<b>Gpa</b>	<b>Giga pascal</b>
<b>Pa</b>	<b>Pascal</b>
<b>Ti-N</b>	<b>Titanium nitride</b>
<b>E<sub>r</sub></b>	<b>the reduced modulus</b>
<b>E<sub>i</sub> and v</b>	<b>The parameters for the indenter</b>
<b>h<sub>max</sub></b>	<b>Maximum displacement</b>
<b>h<sub>f</sub></b>	<b>Final depth</b>
<b>h<sub>i</sub></b>	<b>Intercept displacement</b>
<b>P<sub>max</sub></b>	<b>The highest applied load</b>
<b>A</b>	<b>The contact area</b>
<b>h<sub>c</sub></b>	<b>the contact depth</b>

# General introduction

### General introduction

Surface degradation is one of the most problems damaging and costly in the industry fields. So that it costs an industrialized country every year an equivalent of 3–4% of the GDP, several materials derive their wear and corrosion resistance, which means the formation of a passive film at the surface, any damage to the deposit film during service can be accelerated Corrosion and detachment. Among the many effective techniques developed to eliminate corrosion problems thin-film coating technologies [1].

Thin-films are an effective method of protecting composite and metal and alloy surfaces against environmental attack are also used to augment the lifetime of cutting tools and prevent the degradation of steel by offering a barrier against moisture, oxygen, and other contaminants [2, 3].

Pure titanium is a light, silvery-gray, solid, Bright metal, makes up 0.44 % of the earth's crust is the ninth most abundant mineral in the earth's crust. Among some of its properties, it's Insoluble in water but soluble in concentrated acids, excellent corrosion resistance [4, 5]

The addition of nitrogen to titanium enhances mechanical and tribological properties, and increases significantly the oxidation resistance which is due to the formation of a dense FCC-TiN phase.

Titanium nitride (TiN) is a transition metal and refractory composite with high hardness and good chemical and thermal stability; Moreover (TiN) has a cubic structure of the NaCl type. Titanium nitride (TiN) coatings have a wide field of uses because of their practical characteristics like high hardness, excellent corrosion resistance, and superior wear resistance, so on [6-9]

Thin films are the subject of thousands of new searches because of their interest in modern life and their application in the industrial fields. There is the backbone for most advanced applications like optical devices, energy storage devices, and telecommunications. The thin film is defined as a thin layer of material, their thickness ranging from many nanometers to some micrometers. The structure of thin films is divided into amorphous and polycrystalline structures depending on the methods of preparation and the material nature. Thin films comprise the layer and the substrate where the films are deposited on it. The

morphology of the thin films highly depends on deposition techniques (physical and chemical vapor deposition methods) [10].

This work aims to:

- Explain some basic deposition methods for thin films in detail to give important information for readers about how thin films form.
- Study the influence of nitrogen concentration on the structure and morphological properties, mechanical properties of Ti-N coatings deposited by magnetron sputtering.

This work consists of three chapters:

The first chapter describes some techniques for obtaining the thin films most used in research laboratories and their types, growth processes; we also present literature reviews of titanium and titanium nitride.

In the second chapter, we will present the foundations of (XRD), (EDS) with (WDS) and Scanning electron microscopy (SEM), method of Nanoindentation Techniques' and their various applications.

In the third chapter Ti-N, we present the properties of TiN films prepared by the reactive magnetron sputtering technique with different nitrogen percentages and determine the chemical composition of Ti-N coatings. We also utilized X-ray diffraction analysis to study the influence of N content on the crystal structure of TiN coatings.

Finally, the obtained results were summarized in the general conclusion.

## References

- [1] [https://www.mdpi.com/journal/materials/special\\_issues/Surface\\_Tribocorrosion](https://www.mdpi.com/journal/materials/special_issues/Surface_Tribocorrosion)
- [2] Saji, Viswanathan S., and R. M. Cook, eds. *Corrosion protection and control using nanomaterials*. Elsevier, 2012.
- [3] Hurt, Mark A., and Steven D. Schrock, Chapter 5 - Substantial Maintenance and Rehabilitation, Highway bridge maintenance planning and scheduling. Butterworth-Heinemann, 2016.
- [4] Britannica, the Editors of Encyclopaedia. "Titanium". Encyclopedia Britannica, 4 Nov. 2020, <https://www.britannica.com/science/titanium>. Accessed 20 April 2021.
- [5] "Titanium." Chemicool Periodic Table. Chemicool.com. 18 Oct. 2012. Web. <<https://www.chemicool.com/elements/titanium.html>>.
- [6] Shtansky, D. V., E. A. Levashov, and I. V. Sukhorukova. "Multifunctional bioactive nanostructured films." *Hydroxyapatite (HAP) for biomedical applications*. Woodhead Publishing, 2015. 159-188.
- [7] Valentina K. Prokudina, Titanium Nitride, Editor(s): Inna P. Borovinskaya, Alexander A. Gromov, Evgeny A. Levashov, Yuri M. Maksimov, Alexander S. Mukasyan, Alexander S. Rogachev, Concise Encyclopedia of Self-Propagating High-Temperature Synthesis, Elsevier, 2017, Pages 398-401
- [8] Tominaga, Kikuo, Hideaki Adachi, and Kiyotaka Wasa. "Functional Thin Films." *Handbook of Sputter Deposition Technology: Fundamentals and Applications for Functional Thin Films, Nano-Materials and MEMS (2012)*: 361.
- [9] Jiang, Wei, and Akira Kobayashi. "Research of TiN Coatings by Means of Gas Tunnel Type Plasma Reactive Spraying." *Novel Materials Processing by Advanced Electromagnetic Energy Sources (2005)*: 427-432.
- [10] Jilani, Asim, Mohamed Shaaban Abdel-Wahab, and Ahmed Hosny Hammad. "Advance deposition techniques for thin film and coating." *Modern Technologies for Creating the Thin-film Systems and Coatings 2 (2017)*: 137-149.

# Chapter I

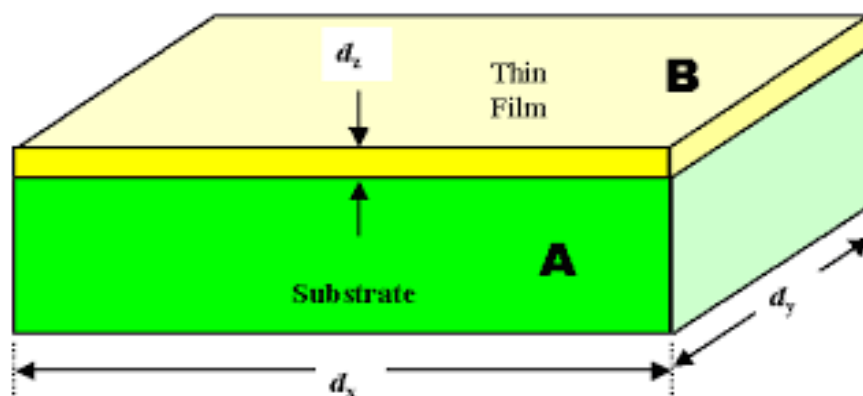
## I.1. Introduction

The hard materials are widely used for protecting the cutting tool and given in economical rise in the industry. However, they are insufficient to support severe mechanical applications (turning, milling, stamping, etc.). Surface treatments remain the adequate solution to improve the performance of a metal surface. These treatments consist of structural transformations, thermo-chemical diffusion treatments and treatments conversion, which improve the performance of new materials obtained after treatment.

Thin films are the subject of new searches due to their interest in lifetime and their exceptional application in the industrial fields. In this chapter, we present some techniques for obtaining thin films used in research laboratories and their growth processes. We present also literature reviews of titanium and titanium nitride.

## I.2. Thin films

Thin films can be defined as (thin layer of material), the thickness is varied from several nanometers to few micrometers. The structure of thin films is varied from amorphous and polycrystalline depending on the preparation condition as well as the material nature. Thin films consist of two parts: the layer and the substrate where the films are deposited on it, as shown in **Figure I. 1** [1]



**I** **Figure I.1.** Schematic of thin film deposited on a substrate. [2]

### I.2.1 Type of thin films

The thin films are very important in the new researchers and exist in many technological fields, such as electronics, optics, mechanics, and decoration so on

### I.2.1.1. Monolayer film

The monolayer coating is a homogeneous film that covers the surface of any material (metallic, polymer, glass) and gives rise to new properties to this material. These coatings are carefully prepared in the 1970s by the vacuum processes. (Figure I. 2 (a)) [3].

### I.2.1.2 Multilayer film

Multilayer are stacks of two (or more) materials repeated successively according to the growth axis. The multilayer film is a proposed a new coating structure, which combines the attractive characteristics of each monolayer (Figure I. 2 (b))[3].

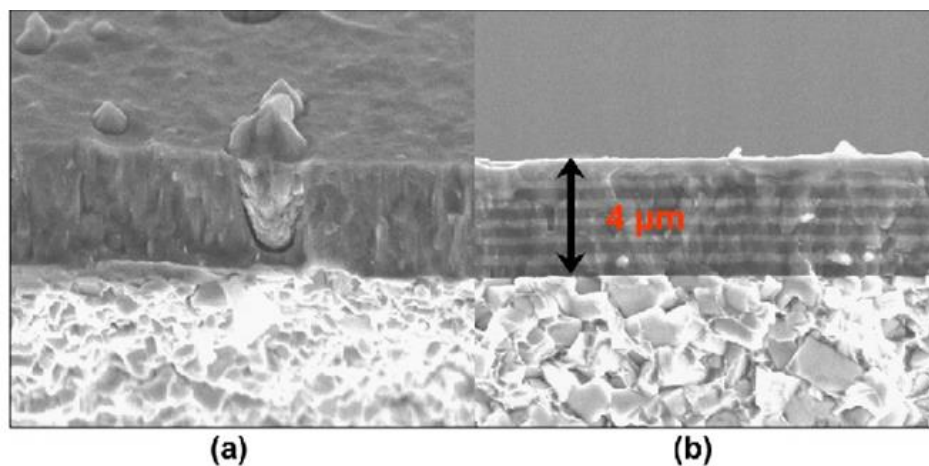
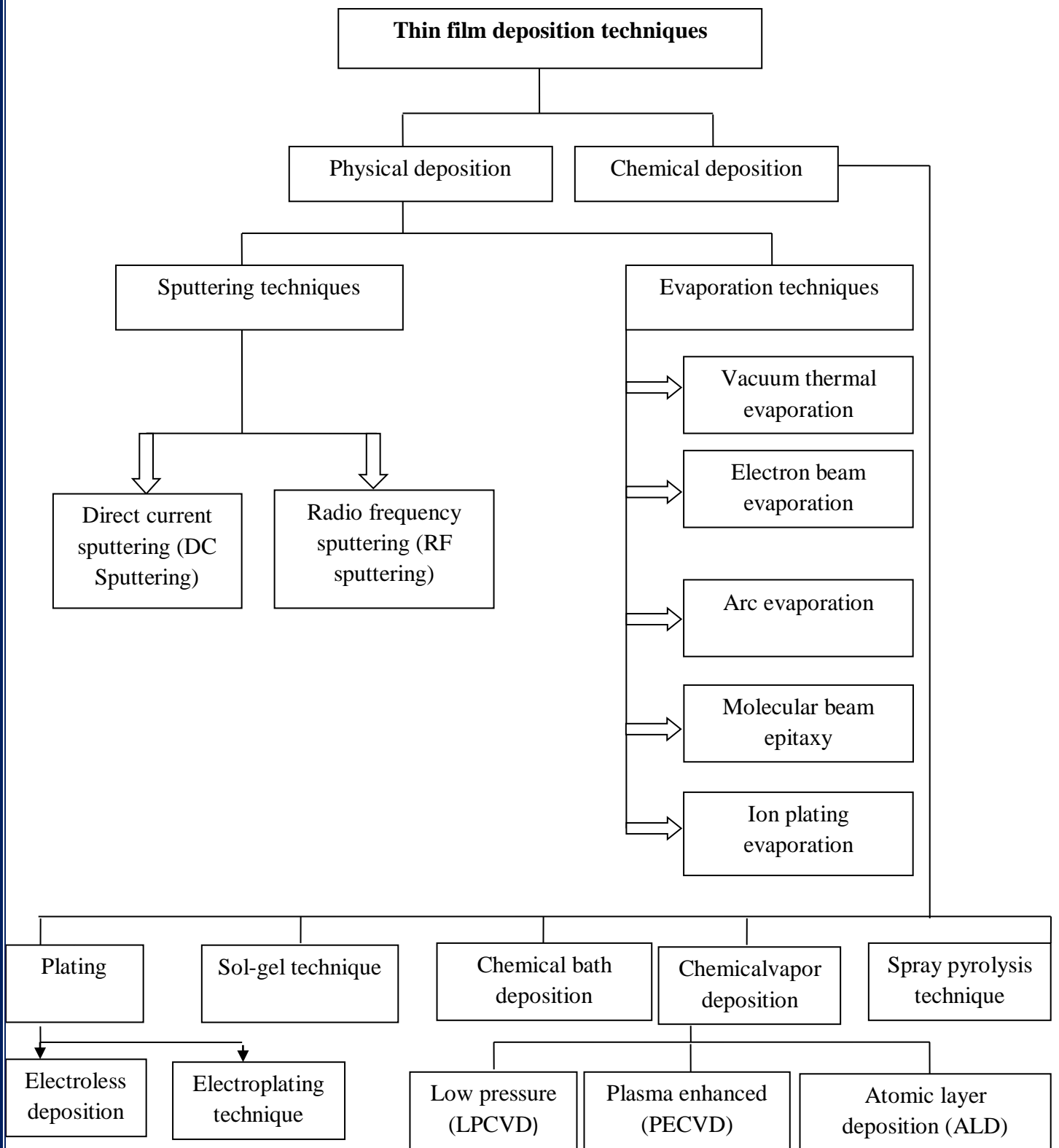


**Figure I.2.** *The structure coatings (a) monolayer (b) multilayer [4]*

### I.3. Deposition technique

In order to obtain thin films with good quality, there are two common deposition techniques: physical and chemical depositions (PVD, CVD). It can be summarized as shown in this schematic.



### I.3.1. Physical deposition techniques

#### I.3.1.1. Evaporation techniques

Evaporation method is considered as the deposition materials films. The obtained film is based by changing the phase of the material from solid phase to vapor phase and converting it to solid on the specific substrate. [1]

##### I.3.1.1.1. Vacuum Thermal Evaporation technique

Vacuum evaporation is the simplest technique utilized to make amorphous thin films such as CdSSe, MnS, Ge-Te-Ga. In This technique there are two parameters: thermal evaporized material and applying a potential to the substrate in the medium or higher vacuum level ranging from  $10^{-5}$  to  $10^{-9}$ mbar (Figure I. 3) [1].

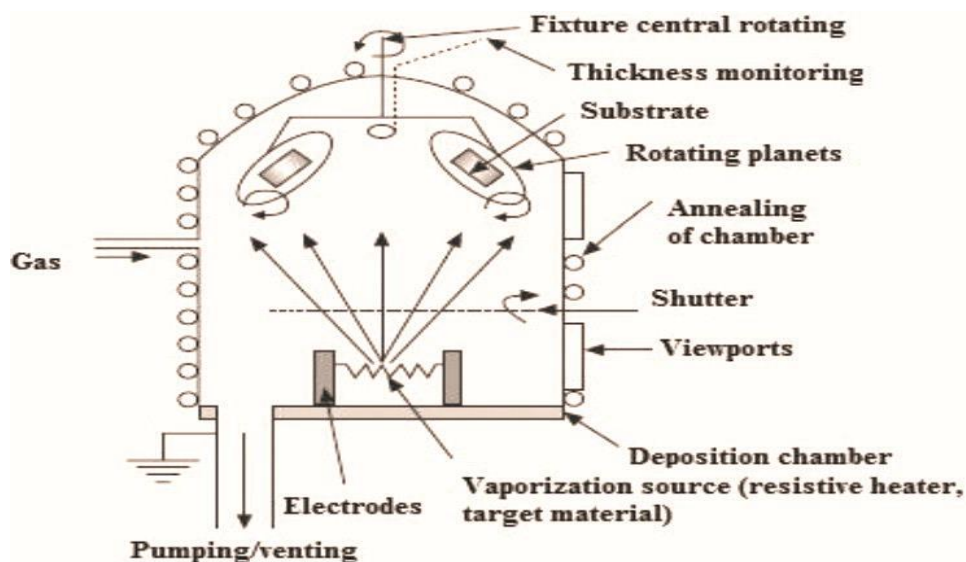


**Figure I.3.** Schematic of thermal evaporation system with substrate holder on a planetary rotation system and directly above the evaporating source [1]

##### I.3.1.1.2. Electron Beam Evaporation

The electron beam evaporated methods is used to the condensation of nonmetals and metals on vacuum. The technological side this method is simple and provides a high growth rates for the coating (up to many micrometers). By heating and bombarding the metals by an electron beam in this process, the material (Figure I. 4). [5]

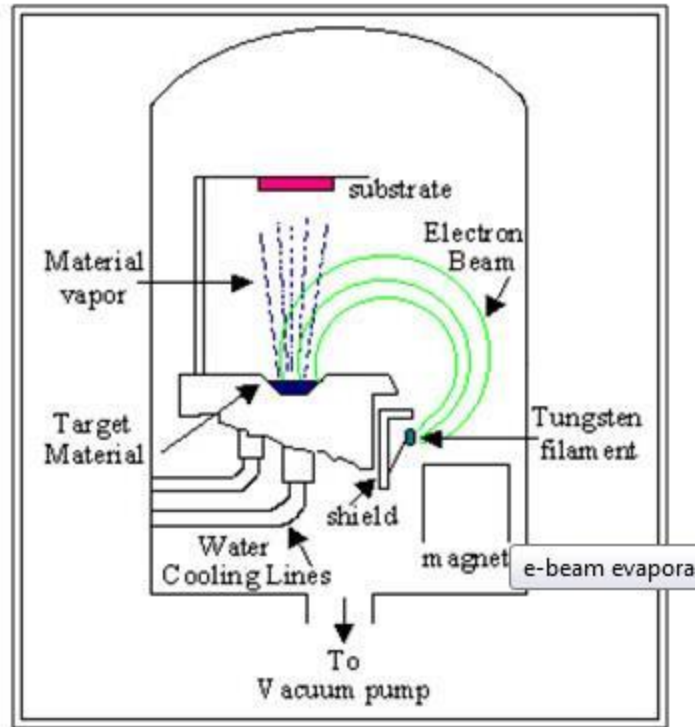


**Figure I.4.** Schematic of electron beam evaporation [6]

#### I.3.1.1.3. Laser beam evaporation (pulsed-laser deposition)

Laser beam evaporation is focused to strike a target of the desired composition at high energy. Then the material was vaporized and deposited as a thin film on a substrate. This process can occur in ultra-high vacuum or in the presence of a background gas, like oxygen when depositing oxides films (**Figure I. 5**) [7].

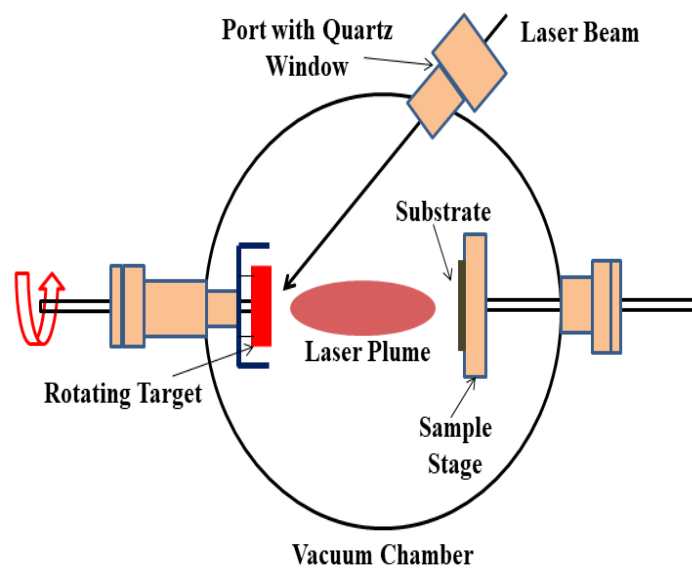


**Figure I.5.** Schematic of pulsed laser deposition technique [8]

### I.3.1.2. Sputtering technique

Several technologies developed for thin film deposition those taken advantages of the sputter phenomenon. The main system used by these technologies consists of a pair of planar electrodes, the anode where the substrate (such as a silicon wafer) is placed and the cathode (the target) which consists of the material that will be used to precipitate the thin film onto the substrate. The electrodes are located inside the vacuum chamber of low pressure ( $\sim 0.1$  Torr) with an inert gas like argon (Ar). By applying, a negative voltage is applied to the target surface, positive Ar ions will accelerate towards the cathode and after falling on it, a small current of atoms or groups of atoms will come out of the cathode material. A small portion of these atoms affect the anode chip to creating a thin layer on the substrate [9]. (See Figure I.6)

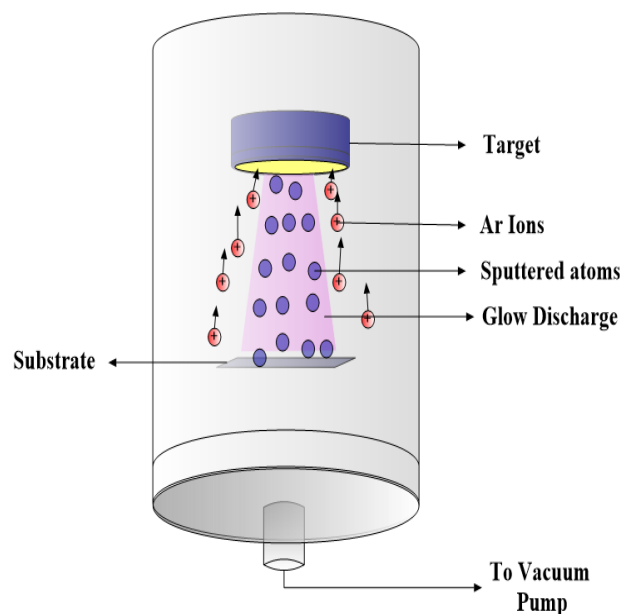


**Figure I.6.** Schematic of the sputtering phenomenon [8]

#### I.3.1.2.1. Direct current sputtering (DC sputtering)

DC (direct current) sputtering is the process of depositing materials used and coating substrate with thin films of various materials. The process involves bombarding a donor material with particles of ionized gas ( $\text{Ar}^+$ ), displacing the donor atoms. These atoms then attached to the negatively charged receptors, forming thin films on the substrate. This technology is widely used for depositing semiconductor components. However, it may be suitable for many other applications, such as non-reflective coatings on optical glass elements, metallic, plastic, packaging materials, and double glazing (**Figure I. 7**).[10]

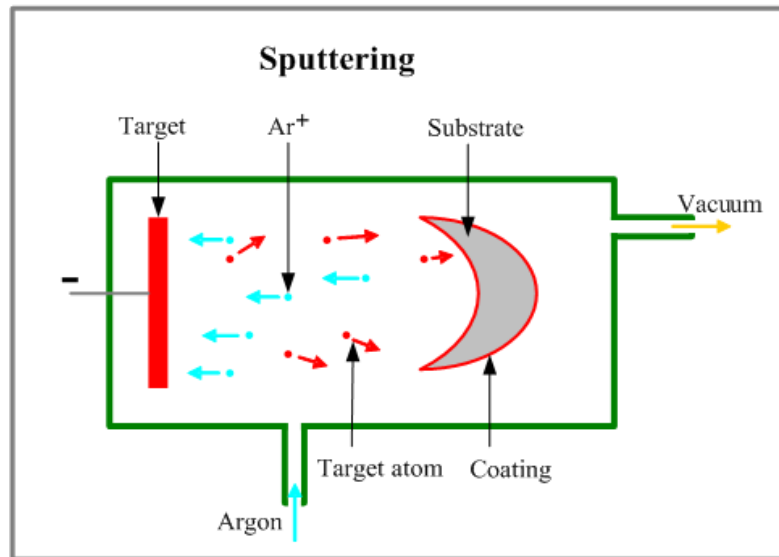


**Figure I.7.** Schematic diagram of DC sputtering [11]

### I.3.1.2.2. Radio frequency sputtering (R. F sputtering)

R.F sputtering process uses an alternate current (AC) power instead of DC power to form an alternating current sputtering system. Since the frequency of the commonly utilized AC power falls in the radio frequency range (5 ~ 30 MHz), this method is called RF sputtering. The R.F sputtering uses positive ions in the radio frequency discharge plasma to bombard the target, and the atoms can be pulverized and deposited on the surface of the substrate to form thin films. The radiofrequency sputtering can be used to deposit almost solid film with high density, high purity, strong adhesion to the substrate, and good process repeatability (Figure I. 8). [12]

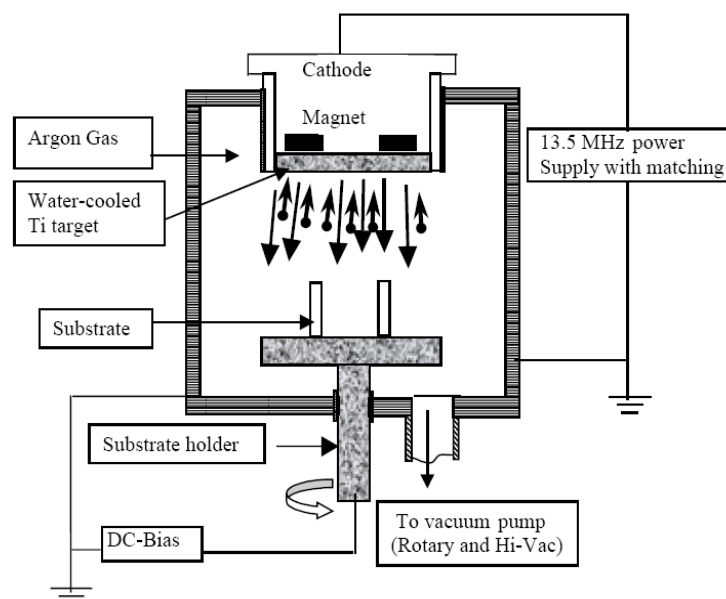


**Figure I.8.** Schematic diagram of radio frequency planar magnetron [13]

### I.3.2. Chemical Deposition Techniques

The chemical deposition technique is economically efficient and industrially used on a wide range. Either thin-film deposition method includes three fundamental steps [5]:

- a) Creation of the proper atomic, molecular, or ionic kinds
- b) Mover of those kinds to the substrate using medium
- c) Condensation on the substrate both direct or through a chemical and electrochemical reaction to form a rigid deposit film.

#### I.3.2.1. Chemical Vapor Deposition (CVD)

These matters are deposited on the heated substrate through the decomposition or chemical reaction of the compounds in the gas that passes over the substrate. Several materials such as silicon nitride, silicon dioxide, amorphous silicon, and single crystalline silicon can be precipitated by the CVD method. A special method in CVD, called Epitaxial Layer Deposition, or Vapor-Phase Epitaxy (VPE), has only one crystal shape as the precipitate. This process is usually performed for specific compositions of substrate and layer materials and under special conditions. In the CVD process, the materials must be in the gaseous or vapor state and react on or near the surface of the substrates at elevated temperatures (Figure I. 9). [14]

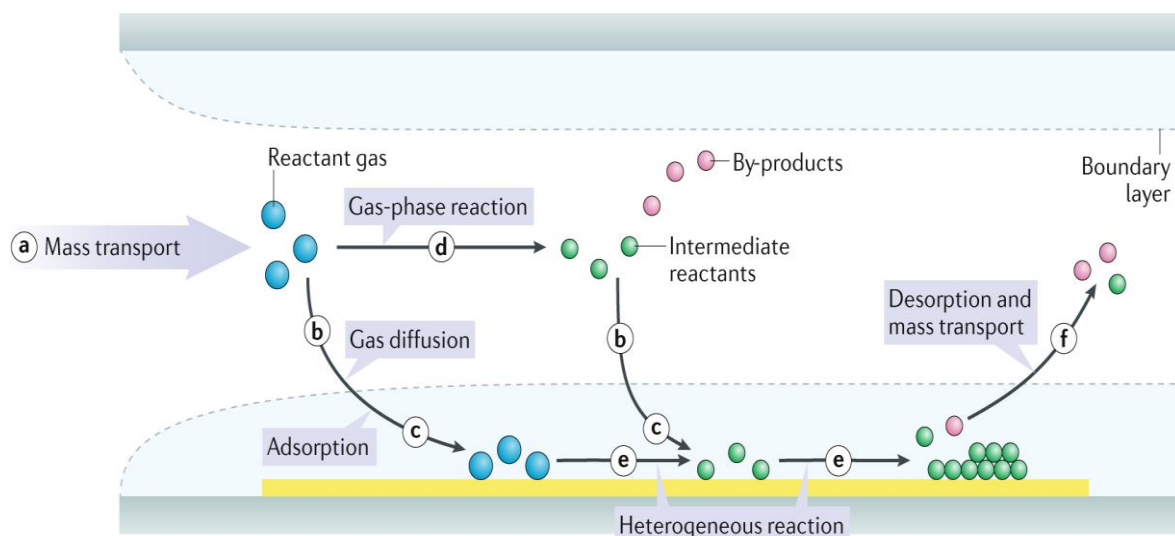


**Figure I.9.** Schematic of general elementary steps of a typical CVD process [15]

### I.3.2.1.1. Low-pressure chemical vapor deposition: LPCVD

LPCVD method is utilized on the deposition of sandwiched semiconductors thin films with few nanometers to many micrometers of thickness. LPCVD is utilized to deposit a wide range of possible film compositions covered with a good matching step. These films include a variety of materials such as poly-silicon for gate contacts, thick oxides films used for isolation, doped oxides for global planarization, nitrides and other dielectrics (Figure I. 10) [16].

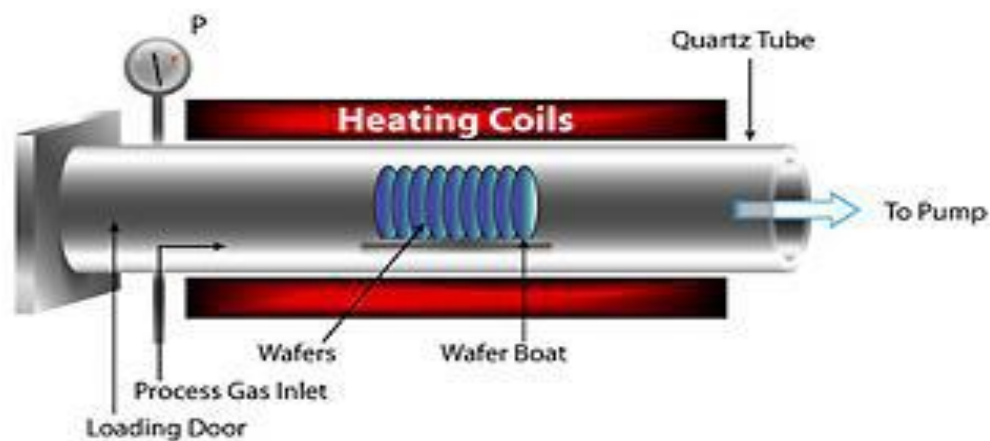


Figure I.10. LPCVD Process [16]

### I.3.2.1.2. Atomic layer deposition (ALD)

The atomic layer deposition is one of deposition technique where the chemical precursors are sequentially insert to the surface substrate and react directly with the surface to form monolayer's film. as the name suggests, a deposition of films on the surface substrate at the atomic scale (Figure I. 11) [17].

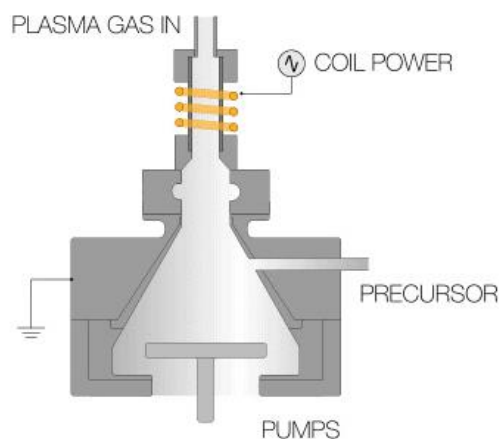


Figure I.11. Atomic layer deposition (ALD) [18]

### I.3.2.2. Chemical Bath Deposition

Chemical bath deposition is one of the solution phase processes beneficial to produce semiconductors composite from aqueous solutions. This method gives several benefits compared to other well-known vapor phase synthetic routes. It permits us to readily control the growth factors like film thickness, deposition rate, and quality of crystallites by changing the solution pH, temperature, and bath concentration. It does not need high voltage devices, operates at room temperature, and so it is an economical process. The only condition for this deposition trajectory is an aqueous solution made up of a little common chemicals and a substrate for the film to be deposited. It usually suffers from a shortage of reproducibility in comparison with other various chemical methods; though, by the appropriate suitable and accurate optimization of the growth parameters, we can reach reasonable reproducibility (Figure I. 12). [5]

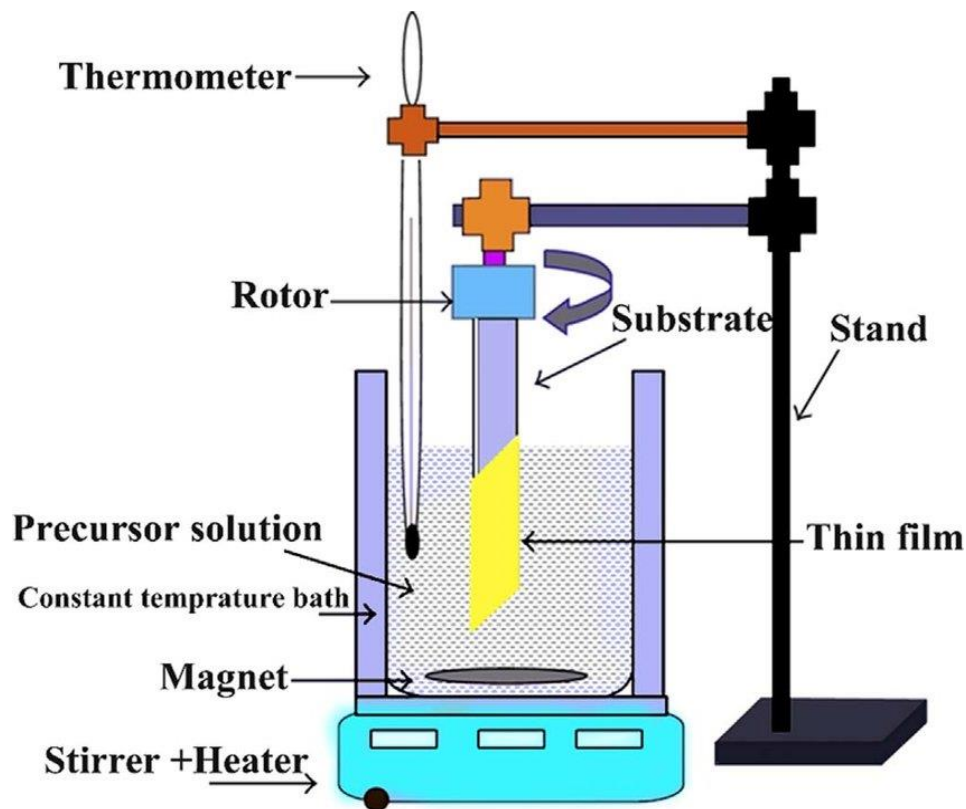
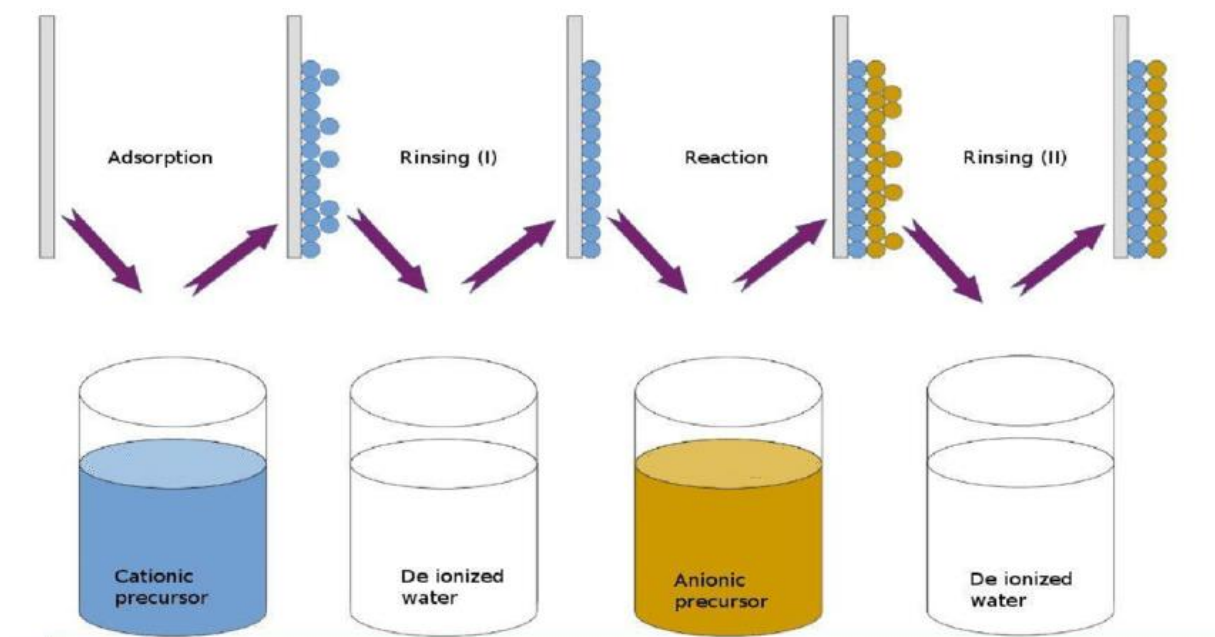


Figure I.12. Experimental set up of CBD technique [19]

### I.3.2.3. Successive Ionic Layer Adsorption and Reaction (SILAR)

Successive ionic layer adsorption and reaction (SILAR) is a new advanced method for the deposition of metal thin layers. This method is depend to the submersion of a substrate in anionic and cationic precursors, accompanied by rinsing of the substrate among each submersion in double-distilled water in order to circumvent homogeneous deposition (Figure I. 13). At the submersion in the cationic precursor, the cations are absorbed into the substrate's surface. The act of rinsing after submerging will separate the unabsorbed or excess ions; while simultaneously preventing homogeneous deposition. Likewise, when submerging in an anionic precursor solution, the anions will interact with the previously absorbed cations. The residual uncreative/powdery material can be ousted thorough rinsing. After some repetitions of these cycles, a multilayer film of wanted thickness will be creating. The quality and thickness of these respective layers are closely related to the preparation parameters (Figure I. 13). [5]



**Figure I.13.** Schematic representation of SILAR method [20]

### I.4. Thin film growth modes

Thin-film growth is a nucleation and growth process containing several steps, such as deposition, diffusion, bonding. Figure I. 14 presents a schematic diagram that explaining the principal atomic processes:

(a) *Deposition of atoms from the vapor on the substrate surface or existing clusters,*

(b) Spread of adatoms on the surface;

(c) Nucleation of adatom clusters,

(d) Addendum of mobile adatoms to the existing clusters,

(e) Dismantling of clusters,

(f) A dynamic balance is getting when the evaporation of the observed atoms from the substrate surface and the deposition of the atoms from the vapor happens at the same time [21].

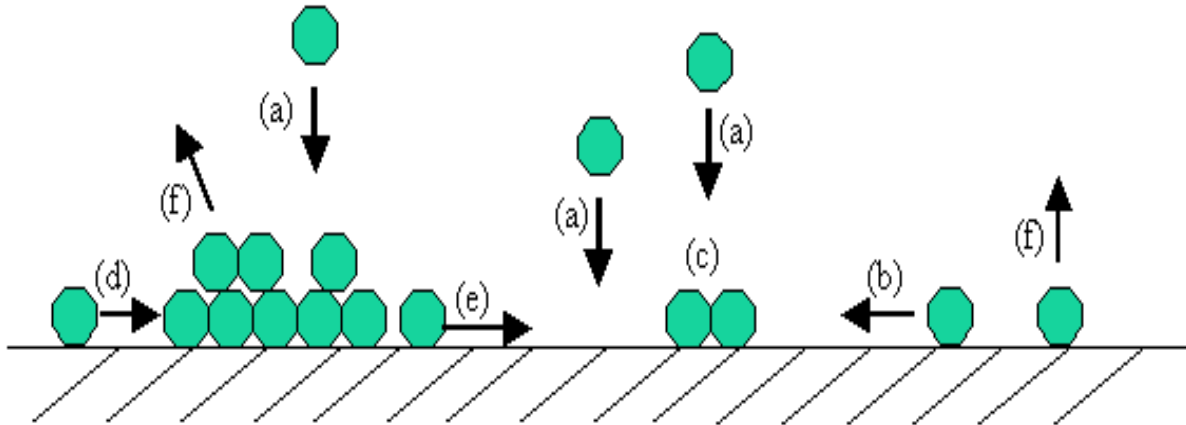


**Figure I.14.** A schematic diagram of thin-film growth steps : (a) deposition of atoms from the vapor (b) surface motion/spread of the adatoms (c) production of clusters by nucleation (d) addendum of adatoms to existing clusters, (e) dismantle of clusters and (f) evaporation. [21]

The film morphology is based on different growth modes of thin-layer on substrates. There are three potential modes of crystal growth on surfaces, *via islet growth, layer-by-layer growth, and a mix growth mode* of the previous two modes.

The film growth mode is directly related to the energy of formation: the surface free energy of the substrate ( $\sigma_s$ ), the surface free energy of the film ( $\sigma_f$ ) and the interfacial energy ( $\sigma_{int}$ ) (between the film and the substrate) that determines the growth mode that a system order takes [21]

#### I.4.1. Island growth mode (Volmer -Weber or V-W mode)

V-W mode indicates the growth mode in which tiny clusters nucleate immediately on the substrate surface and; later grow in three-dimensional isles. Islet growth is a physical method of deposited film growth and chemical vapor deposition. When atoms deposited on a flat surface, random isle walks and meet with any other. Then they make up an isle with a greater mass and a less random walk speed. The size and stabilization of an island will rise as

more atoms are deposited on the substrate and the link with the isle. A high number of separate islets can form and grow independently. Individual islands will grow to become separate grains in the terminal film. This mode is observed in multiple- systems of metal, graphite, and other layer composites such as mica. V-W mode growth occurs when the deposited atoms are strength linked to each other than to the substrate atoms. [21]

#### **I.4.2. Layer-by-layer growth mode (Frank-van der Merwe or F-M mode)**

In F-M mode, little clusters will nucleate and grow into one monolayer in rise in the first step; as the deposition continued, the monolayer Continues growing to form a uniform film. In other meaning, a complete monolayer will compose on the substrate surface before the second layer of film is built up. This growth mode has been seen in several homo-epitaxy systems, like metal on metal; and semiconductor on semiconductor systems. F-M mode growth happens when the deposited atoms are strongly linked to the substrate than to each other. [21]

#### **I.4.3. Layer-by-layer followed by island growth mode (Stranski-Krastanov/SK mode)**

This mode is a mixture of the two former growth modes. Following access a few monolayer's, 3-D islets start to compose on the uniform film, such that the isles are on a "wetting layer", rather than directly on the stripper substrate surface as in V-W growth mode. S-K mode generally seems in heteroe-pitaxial semiconductor systems with a modicum lattice mismatch. It is energetically disadvantageous for the system to continue the layer-by-layer growth. The isle growth mode could avert the formation of misfit dislocations. [21]

. Practically, the film growth mode will be affected by low kinetic parameters:

- (1) The density of adatoms, which is controlled by deposition rate;
- (2) The surface movement of adatoms, which is affected by surface temperature.

The substrate temperature can produces from two sources: either of a local lattice heating by the kinetic energy distribution and the latent heat of condensation or from substrate temperature. Defects, like vacancies, steps, and kinks, will too influence adatom mobility highly. They can act as sinks for propagation atoms, giving them adsorption sites (Figure I. 15). [21]

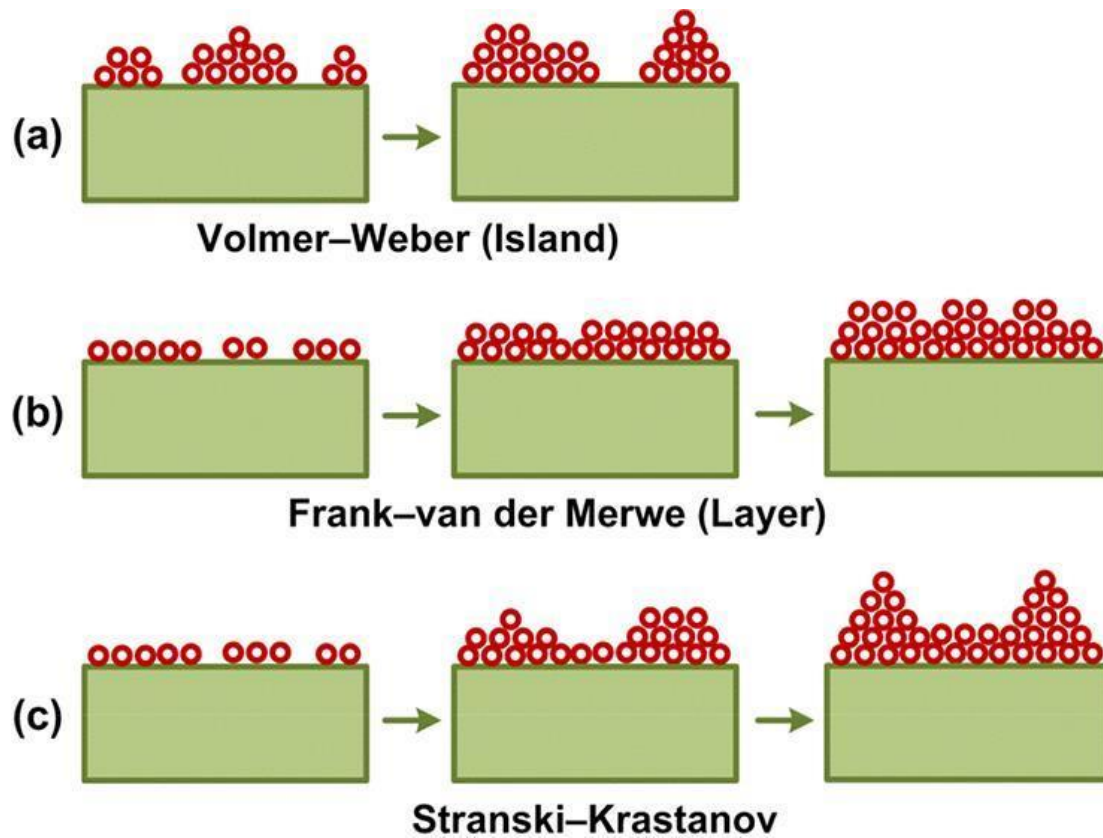


**Figure I.15.** Different thin film growth mechanisms, (a) Island growth model, (b) the layer by layer model, and (c) the mixed growth model [22]

### I.5. Application of thin films

Thin films are utilized for many purposes and in a variety of industries fields such as electro-optical switches, solar energy, and biocompatible coatings on metallic implants.... [23]. Table presents some applications of thin films. [24, 3]

**Table I.1.** Properties and applications of thin film

Fields	Applications
<b>Electrical</b>	Conduction, resistors, piezoelectric sensors, transistors, diodes, antistatic coatings.
<b>Magnetic</b>	Memory discs
<b>Chemical</b>	diffusion barrier, anticorrosion protection or oxidation
<b>Mechanical</b>	reduction of friction, improvement of adhesion, , hardness, Micromechanics
<b>Biomedical</b>	Deposited catalytic coatings, Hydrophilic or hydrophobic films, Anti-reflective coatings, Chemically inert conformal coatings.

## I.6. Titanium

Titanium makes up 0.44 % of the earth's crust is the ninth most abundant mineral in the earth's crust and is found in (all rocks, meteorites and stars); Necessary commercial minerals are ilmenite and rutile. Titanium metal was isolated in pure form by mineralogist Matthew A in 1990 [25].

Titanium (Ti) is a chemical element with atomic number 22, a grayish silver Transition metal from Group II (fourth column, in the transition metals) of the periodic table (**Figure I. 16**) [25, 26].

H																	He
Li	Be	<div style="border: 1px solid black; background-color: #e0f2f1; padding: 5px; display: inline-block; text-align: center;">           22  <b>Ti</b>            Titanium         </div>										B	C	N	O	F	Ne
Na	Mg	<div style="border: 1px solid black; background-color: #e0f2f1; padding: 5px; display: inline-block; text-align: center;">           Atomic Mass 47.87u            Electron Configuration [Ar]4s<sup>2</sup>3d<sup>2</sup>            Oxidation States +4, +3, +2            Year Discovered 1791  <a href="#">View All Properties</a> </div>										Al	Si	P	S	Cl	Ar
K	Ca	Sc	Ti	V	Cr	Mn	Fe	Co	Ni	Cu	Zn	Ga	Ge	As	Se	Br	Kr
Rb	Sr	Y	Zr	Nb	Mo	Tc	Ru	Rh	Pd	Ag	Cd	In	Sn	Sb	Te	I	Xe
Cs	Ba	*	Hf	Ta	W	Re	Os	Ir	Pt	Au	Hg	Tl	Pb	Bi	Po	At	Rn
Fr	Ra	**	Rf	Db	Sg	Bh	Hs	Mt	Ds	Rg	Cn	Nh	Fl	Mc	Lv	Ts	Og
		*	La	Ce	Pr	Nd	Pm	Sm	Eu	Gd	Tb	Dy	Ho	Er	Tm	Yb	Lu
		**	Ac	Th	Pa	U	Np	Pu	Am	Cm	Bk	Cf	Es	Fm	Md	No	Lr

**Figure I.16.** Titanium location in the periodic table [27]

### I.6.1. Discovery of Titanium

Titanium was discovered by the English chemist William Gregor in (1791) and the first pure titanium was produced by American chemist M. A. Hunter in 1910 [25, 28].

### I.6.2. Characteristics

- *Insoluble in water but soluble in concentrated acids*
- *Titanium metal burns in the air at high temperatures and also burns in pure nitrogen.*
- *Good corrosion resistance*
- *Pure titanium is a light, silvery-gray, solid, Bright metal and has a high strength to weight ratio. [29]*

### I.6.3. Crystal Structure

At 882 °C pure titanium displayed an allotropic phase transformation, it transforms from a body-centered cubic (BCC) crystal structure ( $\beta$  phase) at high temperatures to a hexagonal close-packed (HCP) crystal structure ( $\alpha$ ) At low temperatures. The transition temperature depends on the purity of the titanium, which affected by alternate and interstitial elements (**Figurer I. 17**) [30]

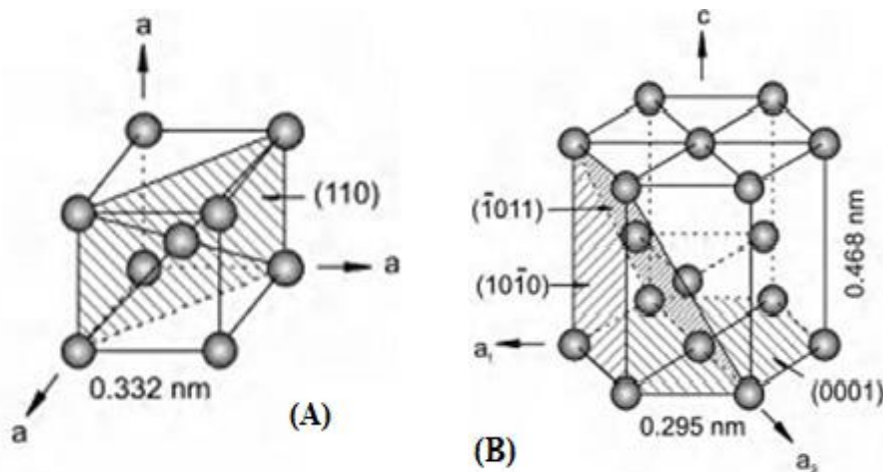
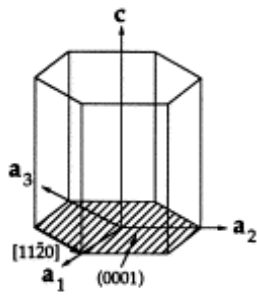


**Figure I.17.** (A)  $\beta$  titanium of BCC.,(B) hexagonal unit cell of the  $\alpha$  phase[31]

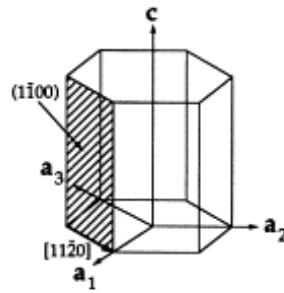
For the (HCP) titanium crystal structure ( $\alpha$ )

- The hexagonal unit cell of the  $\alpha$  phase
- The room temperature values of the lattice parameters  $a=0.295\text{nm}$  ,  $c=0.468\text{nm}$ , as the ideal ratio for a hexagonal packed crystal structure is super than a ratio of pure  $\alpha$  titanium  $1.633 > 1.587$
- It also indicates the sliding systems: (see Figure I.17) [32]
  - ✓ Principal : the  $\{1\ 0\ -1\ 0\} <1\ 1\ -2\ 0>$  planes, called prismatic planes.
  - ✓ Secondary : the  $\{0\ 0\ 0\ 1\} <1\ 1\ -1\ 0>$  planes,It's called the basal plane.

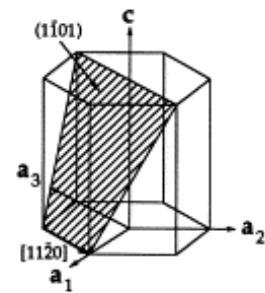
✓ The  $\{1\ 0\ -1\ 1\} \langle 1\ 1\ -2\ 0 \rangle$  and  $\{1\ 1\ -2\ 2\} \langle 1\ 1\ -2\ 3 \rangle$ , called pyramidal planes.



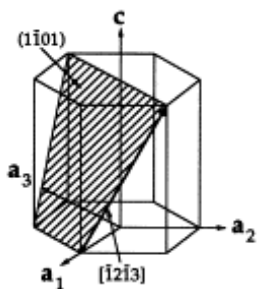
Basal- $\langle a \rangle$   
 $\{0001\} \langle 11\bar{2}0 \rangle$ , 3



Prismatic- $\langle a \rangle$   
 $\{10\bar{1}0\} \langle 11\bar{2}0 \rangle$ , 3



Pyramidal- $\langle a \rangle$   
 $\{10\bar{1}1\} \langle 11\bar{2}0 \rangle$ , 6



1st order Pyramidal- $\langle c + a \rangle$     2nd order Pyramidal- $\langle c + a \rangle$   
 $\{10\bar{1}1\} \langle 11\bar{2}3 \rangle$ , 12                       $\{11\bar{2}2\} \langle 11\bar{2}3 \rangle$ , 6

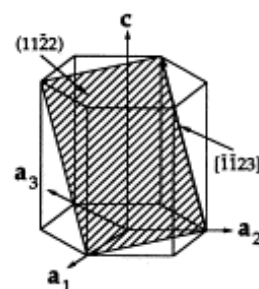


**Figure I.18.** Slip systems[29]

For the (BCC) titanium crystal structure ( $\beta$  phase) (Figure I.18) :[30,31]

- The unit cell of the body-centered cubic (bcc)  $\beta$  phase
- the lattice parameter value of pure titanium At 900 °C:  $a = 0.332$  nm
- The close-packed directions are the four  $\langle 1\ 1\ 1 \rangle$  directions.
- One variant of the six better densely packed  $\{1\ 1\ 0\}$  lattice planes.

#### I.6.4. Properties of titanium

**Table I.2.** Physical Properties [33]

Physical Properties	Values
Melting point	1941K (1668 °C, 3034 °F)
Boiling point	3560 K (3287 °C, 5949 °F)
Heat of fusion	14.15 kJ/mol
Heat of evaporation	425 kJ/mol

Molar heat capacity	25.060 J/ (mol.k)
Density	4.50 g/cm <sup>3</sup>

**Table I.3. Mechanical Properties [34, 35]**

Mechanical Properties	Values
Tensile Strength	220 MPa
Poisson Ratio	0.34
Elastic Modulus of	116 GPa
Hardness (Brinell)	70
Hardness (Vickers)	60
Shear modulus	43.0 GPa
Elongation At Break	54%
Other Mechanical Properties	Ductile
Vapor Pressure At 2000 K	0.98 (Pa)

**Table I.4. Chemical Properties [37, 35]**

Chemical Properties	Values
Chemical Formula	Ti
Electron Work Function	4.33 eV
Electrode potential	0.20 V
CAS number	7440-32-6
Thermal neutron cross section	5.6 barns/atom
Electro-negativity	1.54
Electro-chemical equivalent	0.4468 g/A/h
X-ray absorption edge	2.497 Å
Other Chemical Properties	Ionization, Chemical Stability

**Table I.5 Thermal Properties [34,35]**

Thermal Properties	Values
Molar Heat Capacity	25.06 J/mol·K
Specific Heat	0.52 J/ (kg K)
Thermal Conductivity	21.90 W/m·K
Enthalpy of Fusion	15.48 kJ/mol

Thermal Expansion	8.60 $\mu\text{m}/(\text{m}\cdot\text{K})$
Enthalpy of Vaporization	429.00 kJ/mol
Standard Molar Entropy	27.30 J/mol.K
Enthalpy of Atomization	468.60 kJ/mol

### I.6.5. Isotopes of Titanium

Titanium has twenty-six isotopes, of which five are stable: titanium-46 (8.0 %), titanium-47 (7.3 %), titanium-48 (73.8 %), titanium-49 (5.5 %), and titanium-50 (5.4 %). [25]

### I.6.6. Titanium Uses [34]

- Jewelry industry
- Industry (Chemical, Electrical, Electronic)
- a fundamental of the medical field (Titanium surgical instruments, Hip and knee joints, Wheelchairs, Dental implants)
- Used Titanium tubes in distilleries, submarines, large ships.
- Titanium alloys are used in the Aerospace and war industries.

### I.7. Titanium nitride

Ti-N phase diagram is presented in (Figure 1.18). Proves that there are many phases in this system that are  $\beta\text{Ti}(\text{N})$ ,  $\alpha\text{Ti}(\text{N})$ ,  $\delta\text{TiN}_{1-x}$  and  $\epsilon - \text{Ti}_2\text{N}$ . There are two peritectic reactions existing temperatures 2020 and 2350 °C [36].

**Table I.6.** Phases of titanium nitrides [36]

Phase	Structure	Space Group
$\alpha - \text{Ti}$	Hcp	$P6_3/mmc$
$\beta - \text{Ti}$	Bcc	$\text{Im}\bar{3}m$
$\text{TiN}_{0.26}^*$	Hex.	-
$\text{TiN}_{0.30}^*$	Hcp	$P6_3/mmc$
$\zeta - \text{Ti}_4\text{N}_{3-x}$	Rhomb	R3m
$\eta - \text{Ti}_3\text{N}_{2-x}$	Rhomb	R3m
$\epsilon - \text{Ti}_2\text{N}$	Tetr.	$P4_2/mmc$

$\delta - \text{Ti}_2\text{N}$	Tetr.	$14_1/\text{amd}$
$\delta\text{-TiN}$	fcc (NaCl)	$\text{Fm}\bar{3}\text{m}$

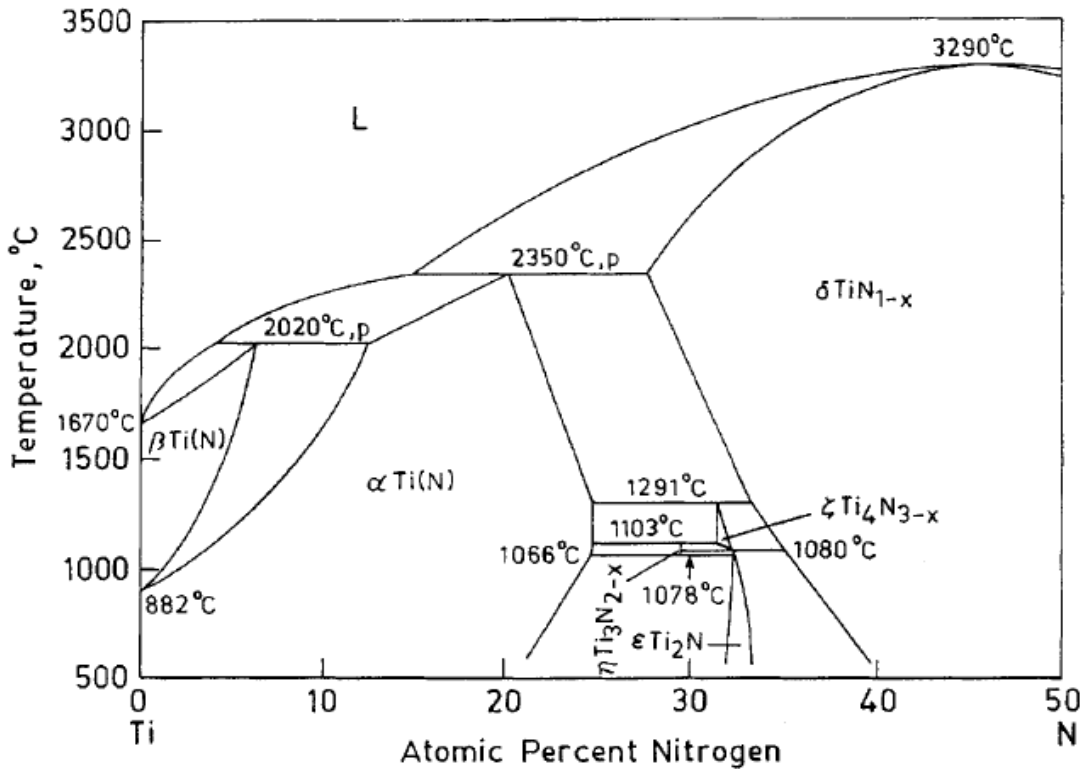


Figure I.19. Ti-N Phase Diagrams [36]

### I.7.1 Structure and properties of titanium nitride

TiN is a refractory interstitial nitride with a golden color, high hardness, high corrosion resistance, and relatively high conductivity. Properties of TiN have been summarized in Table I. 7 and compared to those of Ti. The TiN crystallizes in the rock salt with  $(\text{Fm}\bar{3}\text{m})$ (see Table I.6 and Figure I.19) the titanium atoms are located in the  $(\frac{1}{2}, 0, 0)$  space position of the face-centered cubic, With N, located at all octahedral sites (see Figure I. 20 ), and its lattice parameter is 0.4241 nm, for the stoichiometric TiN phase.[36]

Table I.7. Properties of Ti and TiN, at Room Temperature [36]

Property	TiN	Ti
Structure	fcc (NaCl)	Hcp
Space Group	$\text{Fm}\bar{3}\text{m}$	$\text{p}6_3/\text{mmc}$

Range of Composition	$TiN_{0.6-1.1}$	N/A
Color	Golden	Grey
Density	$5.40 \text{ g/cm}^3$	$4.54 \text{ g/cm}^3$
Melting Point	$2950 \text{ }^\circ\text{C}$	$1940 \text{ }^\circ\text{C}$
Specific Heat	$37.0 \text{ J/mol.K}$	$25.0 \text{ J/mol.K}$
Thermal Conductivity	$30 \text{ Watt/m.K}$	$13 \text{ Watt/m.K}$
Thermal Expansion	$9.36 \times 10^{-6}/K$	$11 \times 10^{-6}/K$
Electrical Resistivity	$20 \mp 10 \mu\Omega. \text{cm}$	$39 \mu\Omega. \text{cm}$
Hall constant	$-6.7 \times 10^{11} \text{ m}^3/C$	$-7.7 \times 10^{11} \text{ m}^3/C$
Vickers Hardness	21-24 GPa	0.55-2.5 GPa
Modulus of Elasticity	612 GPa	110 GPa
Young's Modulus	590 GPa	120 GPa

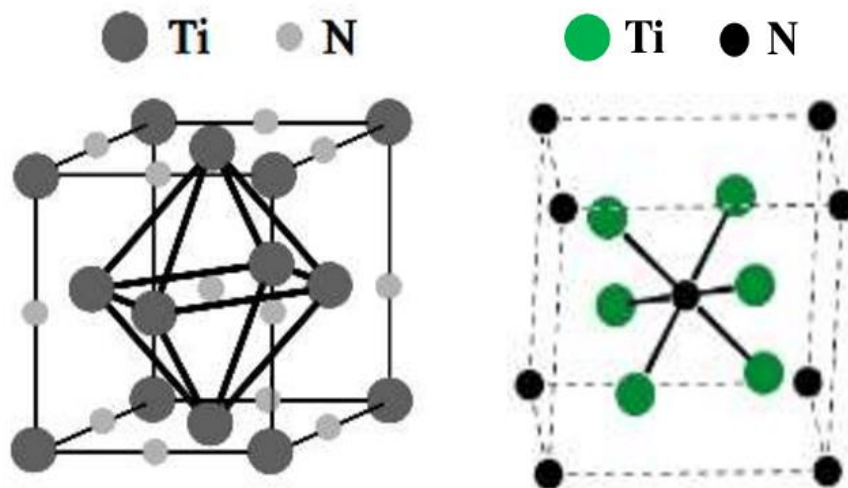


**Figure I.20.** Different polymorphic forms of titanium nitride (left to right:  $\delta$ -TiN and  $Ti_2N$ ) [39]

Titanium nitride has two known intermediate phases  $\epsilon$ - $Ti_2N$  and  $\delta$ - $Ti_2N$  formed at about  $900 \text{ }^\circ\text{C}$ ,

The  $\epsilon$ - $Ti_2N$  phase crystallizes in an "anti-rutile" structure consists of a BCC-Ti lattice, as N atoms does not occupy all of the octahedral sites, but they occupy a half of the octahedral

sites, as opposed to (TiN). (TiN occupies all of the sites octahedral). The unit cell is tetragonal, with  $a$  (4.945 Å)  $c$  (3.034 Å). [36, 40]

**the  $\delta$  – Ti<sub>2</sub>N phase**, An unoccupied ordered form of the rock salt structure with few tetragonal deformations has output symmetry  $14_1/amd$  and nitrogen breaking of  $\sim 38$  at.%. adding N to Ti cause it to transition from the HCP  $\alpha$ -Ti phase to the BCC  $\epsilon$ -Ti<sub>2</sub>N phase and at the end to FCC  $\delta$ -Ti<sub>2</sub>N and  $\delta$ -TiN phases, as expected by the Engel-Brewer theory, The number of valence electrons increases with increasing N fraction. It has been indicated that Ti<sub>2</sub>N phases have a bright yellow color, in contrast to the golden yellow color of TiN. [36]

The properties of TiN are affected by nitrogen fraction and impurities, especially oxygen, as a small amount of oxygen may form unwanted titanium oxides, which may lead to an imbalance in optical properties, hardness and conductivity. Therefore, the restriction of the oxygen content is very important because the free energy to form titanium oxides is favorable for TiN, knowing that these impurities are not limited to oxygen only, as water vapor causes problems similar to those caused by oxygen. Some effort is necessary to determine the nitride phases and impurities are (at least) present, if not the excess composition and microstructure as well. The presence or absence of non-primary stages and a change in the microstructure significantly changes any property in question. [36]

TiN has a density of 5.22 g / cm<sup>3</sup>, with a melting point of TiN is 3203 K at atmospheric pressure, as the mechanical properties of TiN highly depend upon the phases included in the films. Single-phase TiN films were, reported to have stiffness values ranging between  $14.7 \pm 4.9$  GPa and  $34.3 \pm 4.9$  GB and non-stoichiometric films exhibit rigidity values as low as 3.3 GPa. TiN has large bulk and Young's modulus values of 288 GPa and 350 GPa, straight [34]. Ti is a transition metal and has three valence electrons; the basic electrons in the 3d and 4s state are not rigidly bound to the Ti atoms and can speed by an applied electric field. The structure and poorly bonded core electrons in Ti make TiN a conductor. For single-phase TiN films, the electrical resistivity ranging from 18 to  $10^4 \mu\Omega - cm$ . [40]

Often TiN is used as protective, corrosion, and wear-resistant due to its rigidity, chemical, thermal and mechanical stability. It is used as a diffusion barrier layer in microelectronics, Due to electrical connection. TiN thin films often grow with preferred orientations  $\langle 111 \rangle$  and  $\langle 100 \rangle$ , respectively. The preferred direction can be changed from  $\langle 111 \rangle$  to  $\langle 100 \rangle$  by changing the partial pressure N<sub>2</sub> when preparing TiN films with a reactive magnetron sputtering method. It explains this change by the reduction of stress and surface energy. previous work Studied the impact of ion flow and ionic energy on TiN by ion beam-assisted

deposition (IBAD). They reported that the effects of the ion flow between  $\langle 111 \rangle$  and  $\langle 100 \rangle$  could be controlled by regulating ion energy and flow rate [40]

### **I.7.2. Applications**

The application of titanium nitride is very wide due to its physical properties with high melting point, good chemical durability and good conductivity compared to other materials, TiN stands out by two main characteristics; Biocompatibility and CMOS Compliance 8. The TiN coating is used as a protective coating in high temperature environments for applications in supersonic aircraft, 9 and challenging mechanical applications such as grinding tool coating. [41]

### **I.7.3. Effect of nitrogen content on the properties of TiN thin films**

TiN films with different nitrogen contents were prepared to analyze the structural and mechanical features. At high flow rate, the nitrogen content first high slowly from 0 to 8 at %; additionally, the increase of nitrogen flow rate leads to a steep high of the coating nitrogen content up to 50 at %; which corresponds to the stoichiometric TiN compound. XRD diffraction showed the development of the hexagonal  $\alpha$ -Ti phase with a strong [002] direction, where the N atoms taken octahedral sites in the Ti lattice as the quantity of nitrogen is increased, for nitrogen contents of 20 and 30 at.%, the  $\epsilon$ -Ti<sub>2</sub>N phase have a [200] preferential orientation. At higher nitrogen content, the  $\delta$ -TiN phase becomes predominant. When rising nitrogen content, the films become more solid and range from approximately 8 GPa for pure titanium up to 27 GPa for a nitrogen content of 30 at.%. The hardness remains constant with a value of approximately 20 GPa within the range of 45 and 55 at. % N. This is mainly affected by (i): structure/composition (influenced by the processing conditions) and; (ii): the lattice deformation and the increase in stresses. Hardness increases nearly linearly with rising stresses, indicating that lattice deformities and the corresponding increases in intrinsic stresses are important factors for the hardening of the coating[42].

### **I.7.4. Effect of Bias Voltage on the Properties of Ti-N Films**

At use of a negative bias voltage substrate, the deposition of TiN coatings procures structural changes in terms of the film's favored direction, morphology, and mechanical properties [43]. If the thin film is deposited, with increasing substrate bias voltage, the strong TiN (111) was obtain, whereas the direction TiN (200) found at low substrate bias

voltage. the variations in texture of n the TiN films are affected by the following factors: sputtering, ion bombardment, plasma sheath, strain energy, surface free energy, and adatom mobility [43].The deposited nanocrystalline, TiN films stand out as a characteristic pyramidal grain form with crystallite sizes that waning with rising bias voltage, which is proportional to the increasing peak intensity of XRD patterns. Both the surface roughness and the mechanical properties of TiN films were affected by increasing the substrate bias [43]

#### **I.7.5. Temperature effect on the mechanical and tribological properties of titanium nitride thin films**

Regarding the mechanical characteristics, the applying of a negative bias voltage on the substrate raises both modules of elasticity and rigidity, where the values of the modulus of elasticity and rigidity are decreasing when increasing the temperature [44].

### I.8. Conclusion

In this chapter, we reviewed the thin film definition, their properties and applications

We found the deposition process: physical deposition techniques such as (Sputtering technique, Evaporation techniques and so on) and chemical deposition techniques (Chemical Bath Deposition, Successive Ionic Layer Adsorption and Reaction and so on) necessary in the formation of thin films, and the three modes growth

We reviewed the proprieties of Ti-N coatings and the effect of different deposition parameters ;( temperature. base voltage, nitrogen content) on their properties (structural and mechanical properties.

---

**References**

- [1] Jilani, Asim, Mohamed Shaaban Abdel-Wahab, and Ahmed Hosny Hammad. "Advance deposition techniques for thin film and coating." *Modern Technologies for Creating the Thin-film Systems and Coatings 2* (2017): 137-149.
- [2] Ghougali, Mebrouk. *Elaboration and characterization of nanostructuring NiO thin films for gas sensing applications*. Diss. University of Mohamed Khider, BISKRA, 2019
- [3] bensouici fayçal. Universite A. Laghrour – Khenchela, Chapitre I : Introduction à la physique des couches minces et de leurs techniques délaboration.
- [4] Kıvık, Turgay, Gürcan Samtaş, and Adem Çiçek. "Taguchi method based optimisation of drilling parameters in drilling of AISI 316 steel with PVD monolayer and multilayer coated HSS drills." *Measurement* 45.6 (2012): 1547-1557.
- [5] Geremew, Temesgen. "Review of Thin Film Deposition Technique and Its Application." *Review of Thin Film Deposition Technique and Its Application*, 2021.
- [6] Bhowmick, S. H. O. M. N. A. T. H. "Investigation of Pyroelectric Effect Generated by Lithium Niobate Crystals Induced By Integrated Microheaters." (2017).
- [7] <https://www.sciencedirect.com/topics/chemical-engineering/pulsed-laser-deposition>
- [8] Ho, Soon Min, et al. "A review of nanostructured thin films for gas sensing and corrosion protection." *Mediterranean Journal of Chemistry* 7.6 (2018).
- [9] <https://www.brighthubengineering.com/manufacturing-technology/87512-theory-and-operation-of-magnetron-sputter-deposition-coating-process/>
- [10] <https://www.wise-geek.com/what-is-dc-sputtering.htm>
- [11] Prabu, R., et al. "Review of physical vapour deposition (PVD) techniques." *Namakkal India-Proceedings of the International Conference on "Sustainable Manufacturing" ICSM*. 2013.
- [12] <https://www.sputtertargets.net/sputter-coating-technologies-radio-frequency-rf-sputtering.html>

- [13] Prabu, R., et al. "Review of physical vapour deposition (PVD) techniques." *Namakkal India-Proceedings of the International Conference on "Sustainable Manufacturing" ICSM*. 2013.
- [14] <https://www.circuitstoday.com/chemical-vapour-deposition-cvd>
- [15] Sun, Luzhao, et al. "Chemical vapour deposition." *Nature Reviews Methods Primers* 1.1 (2021): 1-20.
- [16] Curley, Ronald, Thomas McCormack, and Matthew Phipps. "Low-pressure CVD and plasma-enhanced CVD." (2018).
- [17] Oviroh, Peter Ozaveshe, et al. "New development of atomic layer deposition: processes, methods and applications." *Science and technology of advanced materials* 20.1 (2019): 465-496.
- [18] [https://plasma.oxinst.com/assets/uploads/3455\\_PLA\\_Plasma\\_Web\\_Banners\\_ALD\\_V3\\_Banner.jpg](https://plasma.oxinst.com/assets/uploads/3455_PLA_Plasma_Web_Banners_ALD_V3_Banner.jpg)
- [19] Dive, Avinash S., et al. "Single step chemical growth of ZnMgS nanorod thin film and its DFT study." *Materials Science and Engineering: B* 228 (2018): 91-95.
- [20] Jose, Edwin, and MC Santhosh Kumar. "Room-temperature wide-range luminescence and structural, optical, and electrical properties of SILAR deposited Cu-Zn-S nano-structured thin films." *Nanostructured Thin Films IX*. Vol. 9929. International Society for Optics and Photonics, 2016
- [21] Sun, Luzhao, et al. "Chemical vapour deposition." *Nature Reviews Methods Primers* 1.1 (2021): 1-20.
- [22] Channam, Venkat Sunil Kumar. *Synthesis of strongly correlated oxides and investigation of their electrical and optical properties*. Diss. 2017
- [23] <https://www.avantes.com/applications/cases/spectroscopy-applications-for-thin-films-and-coatings/>
- [24] Bankoti, Anil Kumar Singh. *Synergistic study on electrochemically deposited thin film with a spectrum from micro to nano range structures*. Diss. 2009.

- [25] Britannica, the Editors of Encyclopaedia. "Titanium". Encyclopedia Britannica, 4 Nov. 2020, <https://www.britannica.com/science/titanium>. Accessed 20 April 2021.
- [26] "What is Titanium? - Properties & Uses." *Study.com*, 27 November 2019, [study.com/academy/lesson/what-is-titanium-properties-uses.html](https://study.com/academy/lesson/what-is-titanium-properties-uses.html)
- [27] National Center for Biotechnology Information. "PubChem Element Summary for AtomicNumber 22, Titanium" PubChem, <https://pubchem.ncbi.nlm.nih.gov/element/Titanium>. Accessed 20 April, 2021
- [28] Ducksters. "Chemistry for Kids: Elements - Titanium." Ducksters, Technological Solutions, Inc. (TSI), [www.ducksters.com/science/chemistry/titanium.php](http://www.ducksters.com/science/chemistry/titanium.php).
- [29] "Titanium." Chemicool Periodic Table. Chemicool.com. 18 Oct. 2012. Web. <<https://www.chemicool.com/elements/titanium.html>>.
- [30] Lütjering, Gerd, and James C. Williams. *Titanium*. Springer Science & Business Media, 2007.
- [31] The Crystal Structure of Titanium, see site: <http://www.metalspiping.com/the-crystal-structure-of-titanium.html>
- [32] [https://material.karlov.mff.cuni.cz/people/strasky/Titanium\\_course/lecture4.pdf](https://material.karlov.mff.cuni.cz/people/strasky/Titanium_course/lecture4.pdf)
- [33] Titanium, see site: <https://www.wikiwand.com/en/Titanium>
- [34] Titanium (Ti) - The Different Properties and Applications. See site: <https://www.azom.com/article.aspx?ArticleID=9118>
- [35] <https://metals.comprenature.com/en/what-is-titanium/model-11-0>
- [36] LeClair, Patrick Royce. *Titanium nitride thin films by the electron shower process*. Diss. Massachusetts Institute of Technology, 1998.
- [37] Structural properties and applications of titanium nitride see site: <https://www.nanotrunk.com/article/structural-properties-and-applications-of-titanium-nitride-i00126i1.html>
- [38] Titanium Nitride (TiN) Nanoparticles - Properties, Applications, see site: <https://www.azonano.com/article.aspx?ArticleID=3372>

- [39] Kanjer, Armand. *De l'efficacité des procédés SMAT et de choc laser dans l'amélioration de la tenue à l'oxydation haute température d'alliages de titane*. Diss. Université Bourgogne Franche-Comté, 2017
- [40] Deniz, Derya. *Texture evolution in metal nitride (aluminum nitride, titanium nitride, hafnium nitride) thin films prepared by off-normal incidence reactive magnetron sputtering*. Diss. University of New Hampshire, 2008.
- [41] Titanium Nitride May 13, 2019 | ACS MATERIAL LLC see site:  
<https://www.acsmaterial.com/blog-detail/titanium-nitride.html>
- [42] Vaz, F., et al. "Influence of nitrogen content on the structural, mechanical and electrical properties of TiN thin films." *Surface and Coatings Technology* 191.2-3 (2005): 317-323.
- [43] Sung-Yong, C. H. U. N. "Bias voltage effect on the properties of TiN films by reactive magnetron sputtering." *Journal of the Korean Physical Society* 56.4 (2010): 1134-1139.
- [44] Merie, V. V., et al. "Analysis on temperature effect on the mechanical and tribological properties of titanium nitride thin films." *IOP Conference Series: Materials Science and Engineering*. Vol. 147. No. 1. IOP Publishing, 2016.

# Chapter II

## II.1. Introduction

In this chapter, we will present the principal characterization techniques such as (XRD), (EDS) with (WDS), Scanning electron microscopy (SEM), and Nanoindentation test and their various applications.

## II.2. X-Ray Diffraction

X-rays are the electromagnetic spectrum among the  $\gamma$ -rays and ultraviolet (UV) radiation, where their energies ranged between 200 eV and MeV [1]. X-ray diffraction is used to determine the size, shape, and internal stress of small crystalline areas; and the average spacing's between layers. It also used to determine the orientation of an individual grain or crystal and identifies the crystal structure of an unknown substance. [2]

X-rays are generated in a cathode ray tube by the interaction of a monochromatic X-ray at a chosen wavelength on the surface of the sample and an incident angle  $\theta$ . The beam is reflected by lattice planes  $\{h, k, l\}$ , discrete by an inter-reticular distance  $d$ , of the crystalline sample. The radiation will excite the vibration of atoms at the same frequency as the X-ray radiation and spread them in all directions. Depending on their orientation, the atoms arranged in the crystal may undergo constructive or destructive interferences, where the constructive interferences or diffraction peaks are determined thanks the Bragg's formulas as shown in (Figure II. 1). [3, 4]

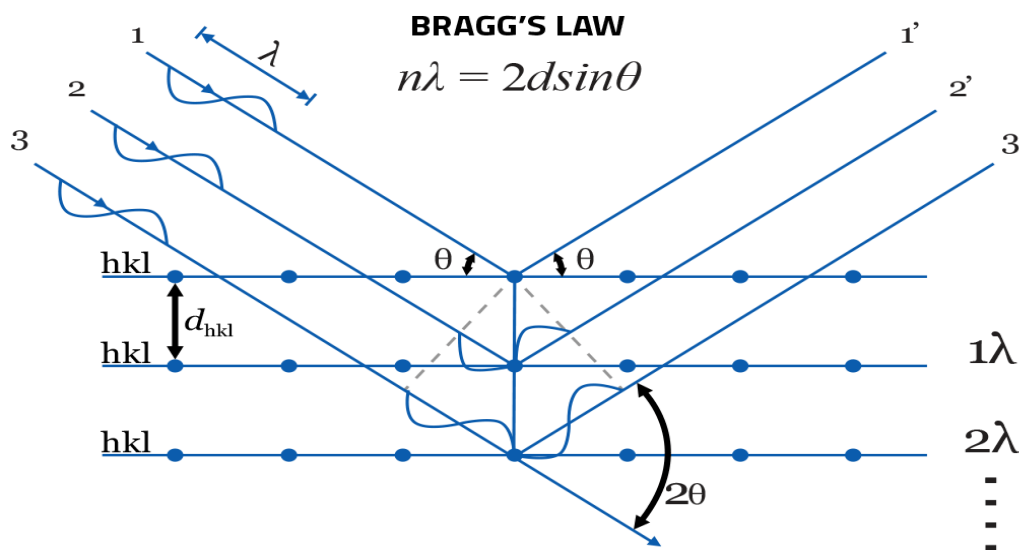


Figure II. 2. Principle of X-ray diffraction [5]

Using the shape and the intensity of the diffracted peaks, angular position, we can access to determine:

- The crystallite size and their distortion, where determined by using the following equation:[1,3]

$$D_{hkl} = \frac{0.94\lambda}{\beta_{hkl}\cos(\theta_{hkl})} \quad \text{II. 1}$$

$d_{hkl}$ : is the average grain size obtaining from the peak (hkl)

$\lambda$  = wavelength of the x-ray

$\theta_{hkl}$ : The angle between the incident ray and the (hkl) scattering planes.

$B_{hkl}$ : full-width-half-maximum of the particular peak.

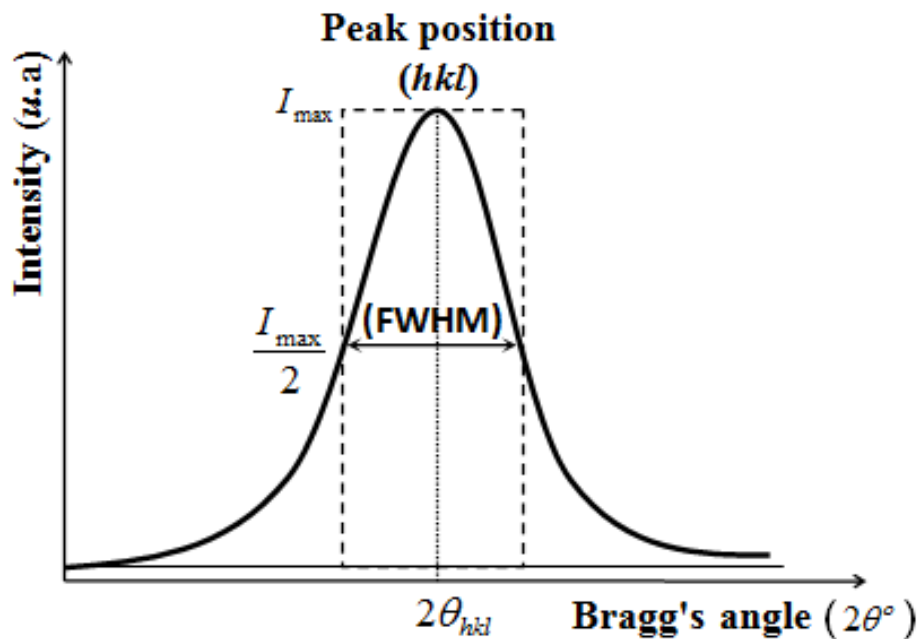


**Figure II. 3.** Full width at half maximum (FWHM) of an arbitrary peak [6]

- The geometry of the crystal, the form and the size of the lattice.[3]
- The type of atoms concerned and their order in the lattice along with their crystallographic direction[3]

### II.2.1. the advantages of XRD

- Fast and effective technique for determining unknown minerals and materials.

- It requires a small sample to analyze.
- Interpreting the resulting data is relatively simple.
- The instruments used to measure x-ray diffraction are widely available.
- Non-destructive technique.[7, 2]

### II.2.2. the X-Ray diffraction equipment

X-ray diffraction is occurred by an X-ray diffractometer, which consists of three important elements. [7]

- X-ray cathode tube
- Sample holder
- X-ray detector

X-Rays are created in a cathode ray tube through a filament are heated to produce electrons, and which are accelerated and directed towards the target by applying voltage, The quickened electrons bombard the target materials to create X-rays; the X-rays are then directed onto the sample.

The X-ray detector in the instrument both rotate, when this geometric movement fulfills the conditions of Bragg's low for the sample being analyzed, constructive interference occurs, causing a peak in intensity. The detector records and processes this signal, converting it into a count rate for output to a computer. [7]

### II.2.3. BRAGG'S LAW

Discover Sir William H. Bragg and his son Sir W. Lawrence Bragg, Bragg's Law in 1913, Bragg's law known in physics as a particular case of Laue diffraction, which determines the angles of coherent and incoherent scattering from a crystal lattice. [8, 9]

The relation between the wavelength ( $\lambda$ ) of the incident X-rays, angle ( $\theta$ ) of incidence, and spacing between the crystal lattice planes ( $d$ ) of atoms is known as Bragg's Law, where this law states that diffraction can happen only when the following equation is satisfied: [9]

$$n\lambda = 2d \sin \theta$$

II.2

$$d_{hkl}^{\text{Cubiccrystal}} = \frac{a}{\sqrt{h^2+k^2+l^2}} \quad \text{II.3}$$

Where:

$\lambda$ : The wavelength of the X-ray,

$d$ : inter-plane distance of (atoms, ions, molecules)

$\theta$ : The incident angle (the angle between incident ray and the scatter plane),  $n$ : an integer is the "order" of reflection

$a$ : Lattice parameter

### II.2.3.1. Derivation of Bragg's Law

Bragg's Law can facilely be derived by considering the conditions necessary to make the phases of the beams match when the incident angle equals and reflecting angle. The rays of the incident beam are always in phase and parallel to each other up to the point at which the top beam hit the top layer at atom z ((Figure II. 3). The second beam continues to the following layer, where it is at point B the second beam dispersion. The second ray must travel the additional distance  $AB + BC$ , known as the integral multiple of the wavelength. If the two beams are continue traveling neighboring and parallel. The distance  $(AB + BC)$  must be an integral ( $n$ ) multiple of the wavelength ( $\lambda$ ) for the phases of the two beams to be the same [10, 11]:

$$n\lambda = AB + BC \quad \text{II.4}$$

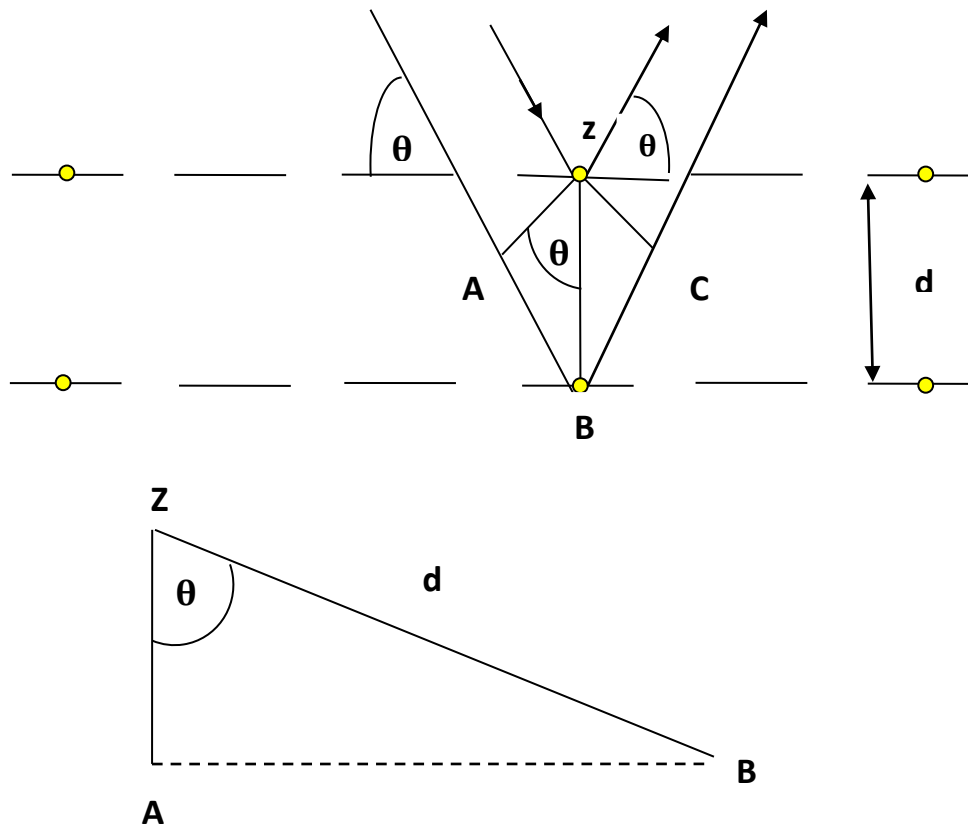


**FIGURE II. 3.** *DERIVING BRAGG'S LAW USING THE REFLECTION GEOMETRY AND APPLYING TRIGONOMETRY [9, 10]*

Through Figure II.3, we find:

$$AB = BC \quad II.5$$

By substituting equation (2.4) in equation (2.3) we find:

$$n\lambda = 2AB \quad II.6$$

ABZ is a right triangle whose hypotenuse is **d**; where we use trigonometry to determine the relationship that connects **d** and theta to distance (**AB + BC**). **AB** is the opposite of the angle  $\theta$ .

$$AB = d \sin \theta \quad II.7$$

So, substituting equation (2.5) in equation (2.6), we find Bragg's equation.

$$n\lambda = 2d \sin \theta$$

### II.2.3.2. Applications of Bragg's Law

There are many applications of Bragg's law in the field of crystallographic science among them: [11]

- In the condition of X-ray fluorescence spectroscopy or Wavelength Dispersive Spectrometry, crystals of known d-spacing are used as analyzing crystals in the spectrometer.
- In XRD the inter-planar spacing or d-spacing of a crystal is used for Description and identification purposes.

### II.3. Microanalyses

X-ray microanalysis is a non-destructive technique that is generally utilized in electron microscopy to complete the composition and distribution of elements in a sample. Under electron bombardment, atoms emit X-rays due to changes in electron states; these x-rays are distinctive for items in the sample. The emitted X-rays can be analyzed utilizing two techniques. Wavelength dispersive X-ray spectroscopy (WDS or WDX) separates the X-rays by diffracting them with crystals, collecting one wavelength, or energy, at a time. In contrast, its sister technique, energy dispersive X-ray spectroscopy (EDS or EDX), collects X-rays of all energies simultaneously

#### II.3.1. Energy-Dispersive X-Ray Spectroscopy (EDS)

X-ray energy dispersive spectroscopy (XEDS, EDS, or EDX) is the fundamental method for executing compositional analysis in the SEM and TEM

An EDS detector comprises a crystal that receives the energy of incoming X-rays via ionization; this leads to the creation of free electrons in the crystal that becomes conductive and create an electrical charge bias. The X-ray absorption transforms the energy of individual X-rays to electrical voltages of relative size; the electrical pulses match the characteristic X-rays of the element [13].

The energy-dispersive (EDS) detector utilizes to disconnect the characteristic X-rays of various elements into an energy spectrum. Among the uses of (EDS) determining the chemical composition of materials and prepare element composition maps across over a much wider raster area, these uses allow set the basic information for the elements [13]

### II.3.1.1. Principles of EDS

The technique depends on the ionization of atoms in the specimen by the expulsion of an inner shell electron by an incident electron. The atom can then repose in several ways, one of which is through the loss of energy by an outer shell electron, which fills the space left behind by the ejected electron. This energy loss results in the emission of an X-ray photon, and the energy of this X-ray is the variation in the energy levels between the ejected and external shell electrons involved. So, the energy of the emitted X-ray is element-specific and can be utilized to give chemical analysis by an energy dispersive detector. Elements existent in concentrations  $> 1\%$  by mass are usually detectable, although mitigating factors like spectral overlap can difficult such detection [15]. (EDS) works best for elements with atomic number ( $Z$ )  $> 3$ [15]. (Figure II. 4)

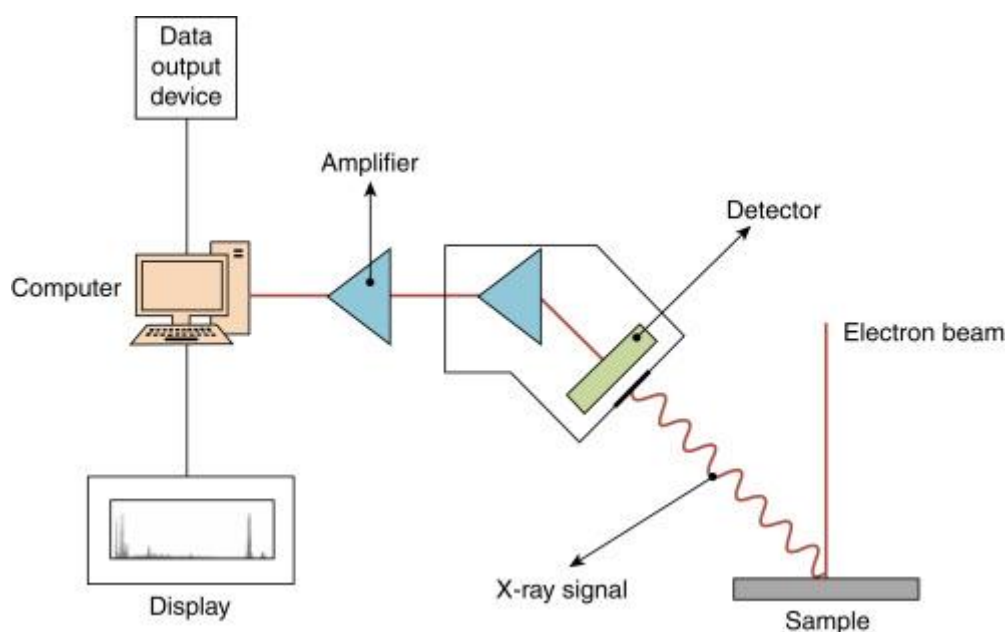


Figure II. 4. Energy dispersive X-ray spectroscopy [16]

### II.3.1.2. EDS analysis applications

- ✓ Product reformulation and competitor analysis
- ✓ Adhesion and bonding investigations
- ✓ Optical appearance, haze and color problems
- ✓ Disputed claim investigations and expert witness

- ✓ Failure investigations, identification of the cause
- ✓ Catalyst quality, poisoning and elemental distribution
- ✓ Product imperfections and defect analysis
- ✓ Contamination detection, isolations and identification
- ✓ Quality control, raw material and end product
- ✓ Filler, pigment, fibre, additive distribution, orientation
- ✓ Assessment of plant particulate emissions
- ✓ Construction and maintenance monitoring (asbestos). [17]

### II.3.2. Wavelength Dispersive Spectroscopy (WDS)

Wavelength Dispersive Spectroscopy (WDS) is a technique for doing x-ray analysis of materials to locate their elemental composition. Elemental analysis by EDS suffers from many weaknesses, which leads to lower detection limits and the incapacity to distribute elements with peaks at comparable energy. WDS overcomes these limitations. It has a much higher energy resolution so that closely spaced peaks can be facilely separated, and it has cleaner background levels so that detection limits are hugely improved over EDS alone. This develops elemental quantification (with the use of appropriate standards) and identification. WDS also has a much greater sensitivity to low atomic number elements, providing much better detection of elements as low as **Be** and **B**. WDS can also be utilized to give two-dimensional elemental distributions as maps [18].

#### II.3.2.1. Principles of WDS

WDS is based on Bragg's Law of diffraction:

$$n\lambda = 2d \sin \theta$$

Where:

$\lambda$  (nm) is the X-ray wavelength of interest

$d$  (nm) is the inter-planar spacing of the diffractometer

$\theta$  is the angle of X-ray incidence on the diffractometer,  $n$  is an integer and

$$E(\text{keV}) = \frac{1.2398}{n\lambda} \quad \text{II.8}$$

[42]

Or

$$E(\text{keV}) = \frac{1.2398n}{2d \sin \theta} \quad \text{II.9}$$

Therefore, the theoretical basis for WDS analysis is quite clear. The material under study generates distinct x-rays. This X-ray diffracted by a diffractometer with well-defined 2D spacing, and diffracted x-rays are calculated using a detector. The geometry of the WD spectrometer is systematically adjusted to select the specific X-ray energy line (s) of interest. The WD spectrometer geometry is mainly modified by changing the angle  $\theta$  of diffraction with respect to the sample. This angle determines the X-ray energy that corresponds to Bragg's law. The characteristic X-ray energy corresponds to a specific element (s). By adjusting the angle of the reflex with respect to the sample, a range of X-ray energies can be analyzed using WDS. The relative intensity of X-rays indicates the relative abundance of the elements present in the sample under study. In this way, WDS is routinely used to quantify elemental concentrations with an accuracy of  $\sim 0.1\%$  (Figure II. 5). [19]

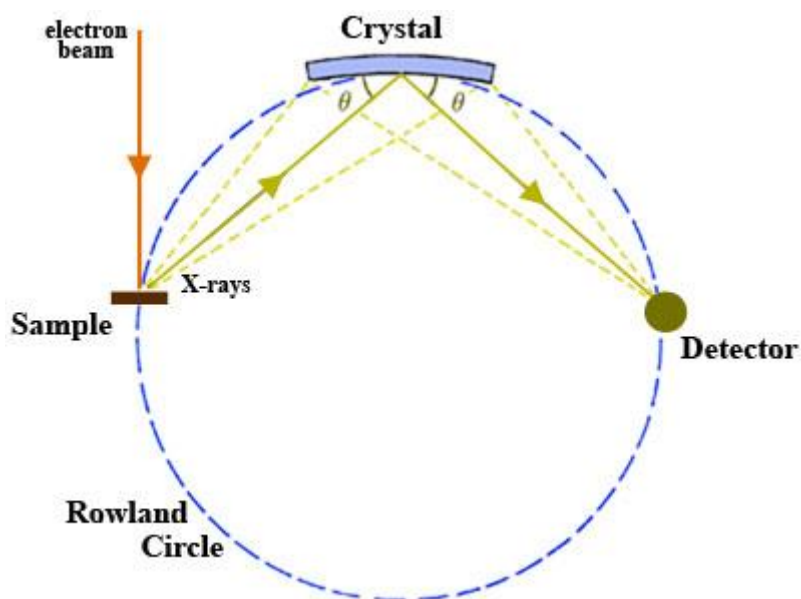


**Figure II. 5.** Configuration of sample, analytical crystal and detector on the Rowland circle within the WD spectrometer

### II.3.2.2. Applications

- Defect identification
- Alloy composition

- *Defects in electronics and electronics packaging.*
- *Mapping low atomic number second phases in steels and other alloys.* [18]

#### II.4. Scanning electron microscopy (SEM)

A scanning electron microscope (SEM) uses a focused beam of high-energy electrons to generate a variety of signals on the surface of solid samples. Signals derived from the reactions of an electronic sample reveal information about the sample including its external appearance (textures), chemical composition, crystalline structure, and orientation of materials making up the sample. In many applications, the obtained data are collected over a selected area of the surface of the sample, and a 2-dimensional image is generated that displays spatial variations in these properties. Areas from about 1 cm to 5  $\mu\text{m}$  wide can be imaged in scanning mode using conventional SEM techniques (magnification ranges from 20 X to about 30000 X, spatial resolution from 50 to 100 nm). The design and functionality of SEM is very similar to EPMA and there is a significant capacity overlap between the two devices (**Figure II.6**). [20]

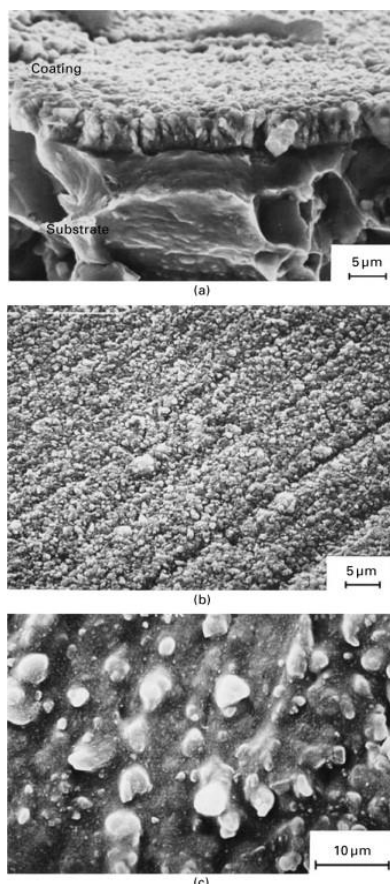


**Figure II.6.** SEM micrographs of titanium nitride coatings: (a) e.b. ion plating, fracture section, (b) e. b. ion plating, coating surface, (c) droplets in arc ion plated TiN[21]

### II.4.1. SEM Principle

In scanning electron microscopy, the electron beam scans the sample in a point pattern. and generated at the upper part of the column by the electron source. These electrons emitted when their thermal energy overcomes the work function of the source material and then accelerated and attraction by the positively charged anode.

The entire electron column needs to be under vacuum. Such as all elements of an electron microscope, the electron source is sealed inside a private chamber to preserve vacuum and protect it from contamination, vibrations, and noise. Besides protecting the electron source from being contaminated, a vacuum also allows the user to get a high-resolution image. In the absence of a vacuum, other atoms and molecules can be present in the column. Their interaction with electrons causes the electron beam to distract and reduces the image quality. High vacuum also increases the collection efficiency of electrons by the detectors that are in the column (Figure II. 7). [22]

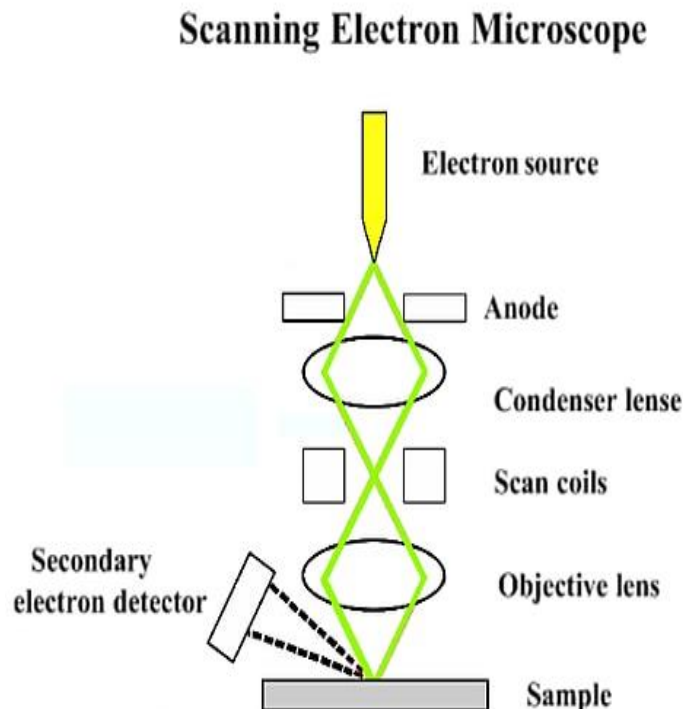


FIGURE II. 7. BASIC COMPONENTS OF AN SEM [22]

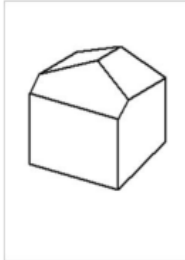
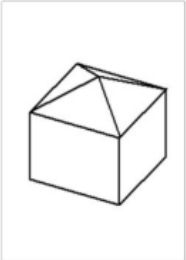
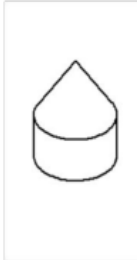
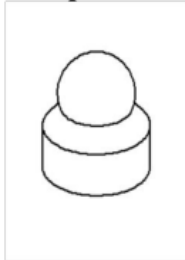
## II.5. Nanoindentation

### II.5.1 Definition

Nanoindentation is a method for examining the hardness and related mechanical properties of materials, simplified by high-accuracy appliances in the nanometer scale, In addition to analytical and computational algorithms for result evaluation [23]

### II.5.2. Nanoindentation Principles

At the essence of the Nano center is a tiny probe bearing a calibrated internal tip; this probe may have a specific shape, such as pyramidal or flat (as illustrated in Figure II. 8) this is used to examine the material surface and measure subsequent force-displacement data [24].

Berkovich	Vickers	Cone	Sphere
			
<ul style="list-style-type: none"> <li>• Bulk Materials</li> <li>• Thin Films</li> <li>• Polymers</li> <li>• Scratch Testing</li> <li>• Wear Testing</li> <li>• MEMS</li> <li>• In-situ Imaging</li> </ul>	<ul style="list-style-type: none"> <li>• Bulk Materials</li> <li>• Films and Foils</li> <li>• Scratch Testing</li> <li>• Wear Testing</li> </ul>	<ul style="list-style-type: none"> <li>• Scratch Testing</li> <li>• Wear Testing</li> <li>• In-situ Imaging</li> <li>• MEMS</li> </ul>	<ul style="list-style-type: none"> <li>• MEMS</li> </ul>

**Figure II. 8.** Most common tip geometries and corresponding applications[25]

Conventional Nanoindenters are mostly load-controlled devices where their tip in contact with the surface under a predetermined load. Once the Nanoindenter has related the specimen, the load augmented and the tip indents in the material. The region of connection between the tip and the specimen, the applied force of the nanoindenter, and the depth of displacement are n utilized to locate the material's mechanical properties. [24].

Traditionally, the size and depth of the residual indentation imprint are taken to determine the material's solidity. This is characterized according to one of many indentation solidity scales,

including the Vickers and Brinell scales. nanoindenters have demonstrated its value for micro-solidness testing where specimens are thick or thin, and they have also explained unique execution for measurements where the microstructural properties of a specimen are complex or non-homogenous (Figure II. 8)[26]

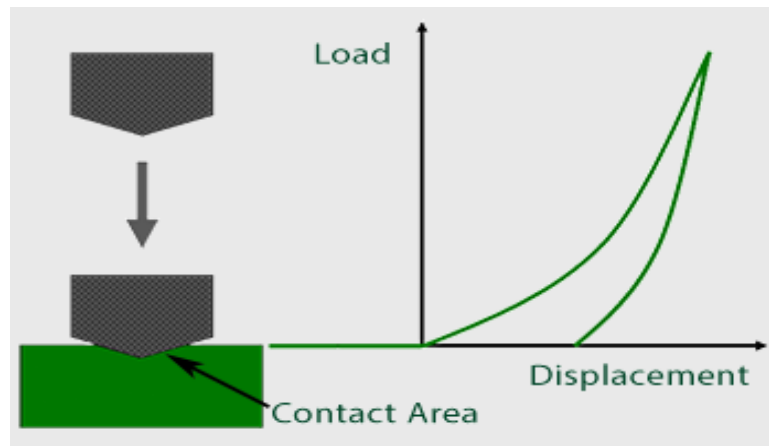


FIGURE II. 9. SCHEMATIC OF AN INDENTATION TEST [26]

### II.5.3. Applications of Nanoindentation

Nanoindentation is utilized for testing local mechanical properties of the hard thin films with very little residual impressions. Conventional techniques are somewhat incapable of testing small-sized components. in the state of coatings, a nanoindenter exam the properties of very thin film thickness  $< 1 \mu\text{m}$  without any effect from the properties of the substrate underneath [24].

### II.6. Hardness and Young's modulus

Hardness is a measure of how resistant a solid is to several form changes when a compressive force is applied [27].It is also called the highest applied load  $P_{max}$ divided by the corresponding contact region  $A$  [25].

$$H = \frac{P_{max}}{A(h_c)} \quad II.10$$

Where:

$P_{max}$  is the peak indentation load its measurement from the load-displacement curve (Figure II. 9), the contact region  $A$  is calibrated empirically as a function of the contact depth  $h_c$ .

Determination of ( $h_c$ ) depends on the presumption that the contact periphery of the indented region behaves like a hard punch on a flat elastic half-space, sinking in during penetration as shown in (Figure II. 10) [25].

There is several measurement techniques are used to determine hardness on both the macro and micro scales. These techniques often rely on measuring the penetration resistance of a material to permanent deformation by a special indenter. The two most usually utilized micro-hardness tests in the state of thin-film measurements are: [27]

- 1) Vickers hardness test (HV)
- 2) Knoop hardness test (HK)

During the exam, an indenter with known geometry is pressed in the material with a fixed load and the deepness of breakthrough is utilized for calculation of the solidness of examined material a typical load-displacement curve is shown in Figure II. 9 [27]

$$\frac{1}{E_r} = \frac{1-\nu^2}{E} + \frac{1-\nu_i^2}{E_i} \quad \text{II.11}$$

To remove the elastic contribution to the displacement and located the projected area from the load-displacement curve the Oliver and Pharr model can be utilized. [27]:

$$S = \frac{dP}{dH} = \frac{2}{\sqrt{\pi}} E_r \sqrt{A} \quad \text{II. 12}$$

Where:

$S = \frac{dP}{dH}$ : is the experimentally measured stiffness of the upper portion of the unloading data [28]

$E_r$ : Is the reduced modulus [28]

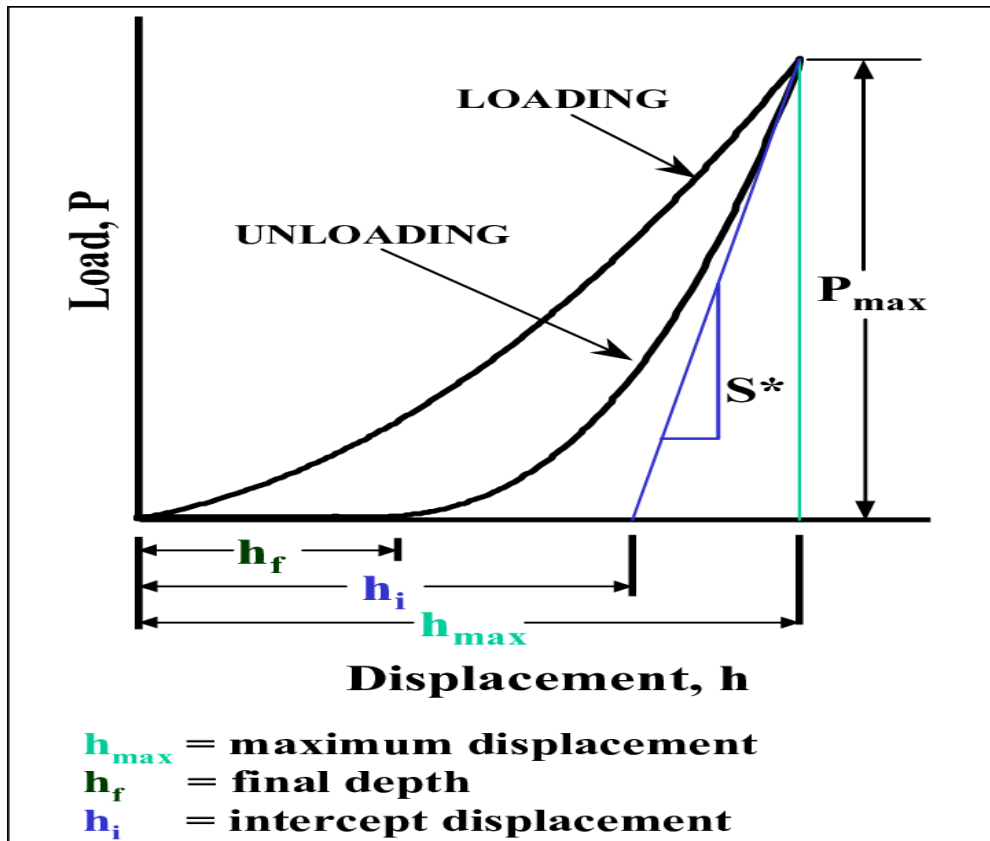


FIGURE II. 10. SCHEMATIC OF THE LOAD-DISPLACEMENT CURVE[28]

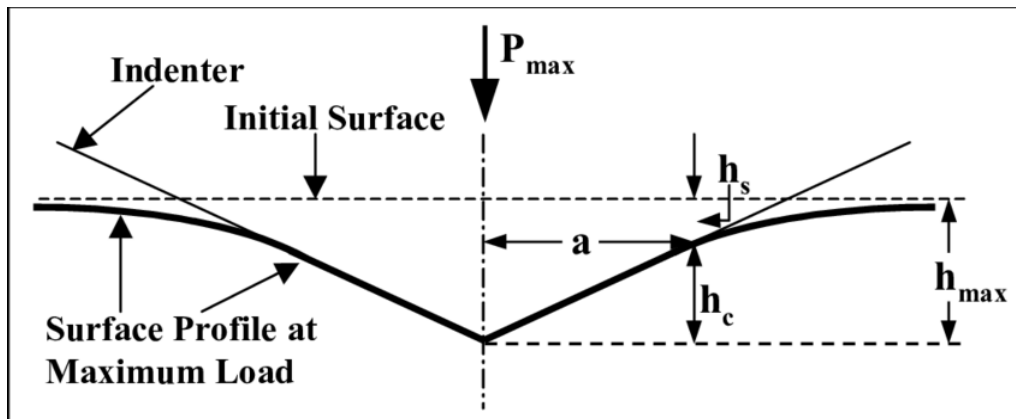


FIGURE II. 11. CONTACT GEOMETRY PARAMETERS [28]

The elastic modulus is defined as [27]:

$$\frac{1}{E_r} = \frac{1-\nu^2}{E_r} + \frac{1-\nu^2}{E_i} \quad II.13$$

The reduced modulus is defined as [28]:

$$E_r = \frac{S\sqrt{\pi}}{2\beta\sqrt{A}}$$

*II.14*

Where:

$\beta$ : is a known dimensionless constant [27]

$\nu$ : the Poisson's ratio of the film[27]

$E_i$  and  $\nu_i$  are the same parameters for the indenter [27].

## II.7. Conclusion

In this chapter, we defined and explained the methods of characterization that used in this work: (such as XRD) to define the crystal structure of samples; and determining the chemical composition of the material and the fundamental information for the elements by an energy-dispersive (EDS) detector and Wavelength Dispersive Spectroscopy (WDS)

We presented the principle, characteristics and applications of the Nanoindentation method to examine both the hardness and young modulus of the materials.

---

**References**

- [1] Melk, Latifa. "Thermal Analysis of Hard Ceramics." (2011).
- [2] <https://www.veqter.co.uk/residual-stress-measurement/x-ray-diffraction>
- [3] Gharbi, Oumaïma. In-situ investigation of elemental corrosion reactions during the surface treatment of Al-Cu and Al-Cu-Li alloys. Diss. Paris 6, 2016.
- [4] Hossain, Shaikh Tofazzel. Synthesis and kinetic study of CeO<sub>2</sub> and SiO<sub>2</sub> supported CuO catalysts for CO oxidation. Diss. 2018.
- [5] <https://www.veqter.co.uk/residual-stress-measurement/x-ray-diffraction>
- [6] Ghougali, Mebrouk. Elaboration and characterization of nanostructuring NiO thin films for gas sensing applications. Diss. University of Mohamed Khider, BISKRA, 2019.
- [7] <https://www.scimed.co.uk/education/what-is-x-ray-diffraction-xrd/>
- [8] <https://www.slideshare.net/MetallurgicalFacts/braggs-law-104917175/3>
- [9] [https://serc.carleton.edu/research\\_education/geochemsheets/BraggsLaw.html](https://serc.carleton.edu/research_education/geochemsheets/BraggsLaw.html)
- [10] <http://skuld.bmsc.washington.edu/~merritt/bc530/bragg/>
- [11] <https://byjus.com/physics/braggs-law/>
- [12] [http://www.laborexport.hu/\\_data/VFS\\_be564080af6d6a2942db1be5b9743e39.PDF](http://www.laborexport.hu/_data/VFS_be564080af6d6a2942db1be5b9743e39.PDF)
- [13] [https://serc.carleton.edu/research\\_education/geochemsheets/eds.html](https://serc.carleton.edu/research_education/geochemsheets/eds.html)
- [14] Holbrook, R. David, et al. "Overview of nanomaterial characterization and metrology." *Frontiers of Nanoscience*. Vol. 8. Elsevier, 2015. 47-87.
- [15] Lu, Shifeier. *Analytical study of osteoporosis of maxilla in ovariectomized rats*. Diss. Queensland University of Technology, 2015.
- [16] Colpan, Can O., Yagmur Nalbant, and Mustafa Ercelik. "4.28 Fundamentals of Fuel Cell Technologies." (2018): 1107-1130.
- [17] <https://www.intertek.com/analysis/microscopy/edx/>
- [18] <http://analyticalanswersinc.com/wp-content/uploads/2016/10/Wavelength-Dispersive-Spectroscopy-EDITED.pdf>
- [19] White, P. "Principles and Applications of Parallel Beam Wavelength Dispersive X-ray Spectroscopy."
- [20] [https://serc.carleton.edu/research\\_education/geochemsheets/techniques/SEM.html](https://serc.carleton.edu/research_education/geochemsheets/techniques/SEM.html)
- [21] Ashrafizadeh, F. "Plasma-assisted surface treatment of aluminium alloys to combat wear." *Surface Engineering of Light Alloys*. Woodhead Publishing, 2010. 323-361.

- [22] <https://www.thermofisher.com/blog/microscopy/what-is-sem-scanning-electron-microscopy-explained/>
- [23] Michailidis N., Bouzakis KD., Koenders L., Herrmann K. (2014) Nanoindentation. In: C.I.R.P., Laperrière L., Reinhart G. (eds) CIRP Encyclopedia of Production Engineering. Springer, Berlin, Heidelberg.
- [24] <https://alemnis.com/what-is-a-nanoindenter/>
- [25] de Vasconcelos, Luize Scalco. *High-throughput mechanical characterization methods for composite electrodes and in-situ analysis of Li-ion batteries*. Diss. Purdue University West Lafayette, 2016.
- [26] <https://www.nanoscience.com/techniques/mechanical-testing/>
- [27] Zenkin, Sergei. "Disertační práce." (2017).
- [28] VanLandingham, Mark R., et al. "Nanoindentation of polymers: an overview." *Macromolecular symposia*. Vol. 167. No. 1. Weinheim: WILEY-VCH Verlag GmbH, 2001.

# Chapter III

### III.1. Introduction

In this chapter, Ti-N coating films were prepared by the reactive magnetron sputtering technique with different nitrogen percentages and determine the chemical composition of Ti-N coatings by EDS. We also utilized x-ray diffraction analysis to study the influence of N content on the crystal structure of TiN coatings.

### III.2. Experimental details

Titanium nitride coatings were deposited by magnetron sputtering at different nitrogen percentage on Si (100) and XC100 substrates. A circular Ti (99.99 % purity) target (D = 200 mm diameter, e = 6 mm) was used. The substrates were polished and cleaned in acetone and ethanol, dried, and then fixed on the substrate-holder. Prior to the film deposition, the Ti target was etched by Ar ions bombardment for 10 min. The films were deposited under different N<sub>2</sub> partial pressures and the deposition conditions were listed in Table III. 1.

**Table III. 1:** deposition conditions for TiN coatings deposited by R.F magnetron sputtering with different nitrogen percentages.

<b>Percentage (Ar, N<sub>2</sub>)</b>	(75 %, 25 %), (80 %, 20 %), (85 %, 15 %), (90 %, 10 %), (95 %, 5 %).
<b>Applied Tension to Ti Target</b>	-900 V
<b>Distance Target-substrate</b>	80 mm
<b>Applied power to Ti Target</b>	650 W
<b>Time</b>	120mn.
<b>Pressure</b>	0.4 Pa.
<b>Substrates</b>	Si <100>, XC100.
<b>Etching (Si, XC100)</b>	5mn

### III. 3. Results and discussion

#### III. 3.1. Chemical composition of TiN coatings

The chemical composition of Ti-N coatings deposited under different nitrogen percentage were determined by EDS and listed in Table III. 2. Ti-N film deposited under 5 % of N<sub>2</sub> presented low nitrogen content and N/Ti ratio is around 0.17, which lead to form a pure Ti phase as observed in chromium nitride coatings deposited by the same process [1]. With increasing the nitrogen flow rate clearly led to a considerable increase in the nitrogen content from (14 to (54) at. % and to a decrease of titanium from 87 to (43 at.% as seen in Table III. 2. The decrease of titanium with increase in the nitrogen content was reported in previous studies for other transition metal nitrides coatings [2]. At 20 %, the (N/Ti ratio with 1.05 was consistent with the stoichiometric of TiN phase [3]. a low amount of oxygen (2-5 at.%, ) was detected in all TiN coatings due to the residual oxygen in the vacuum chamber.

**Table III. 2.** Chemical composition, film thickness, lattice parameter, grain size of the TiN coatings.

N <sub>2</sub> %	Chemical composition at.%				Film thickness μm	Lattice parameter nm	Grain size nm
	N	Ti	O	N/Ti			
5	10	87	3	0.17	1.80	0.0303	87
10	21	74	5	0.28	1.54	0.8402	79
15	32	65	3	0.49	1.45	0.6369	77
20	48	49	3	0.98	1.26	0.7662	64
30	54	43	3	1.25	0.97	0.5360	79

#### III. 3.2. Crystalline structure

The X Ray Diffraction analysis was used to study the effect of N content on the crystal structure of TiN coatings and the results are shown in Figure III. 2.

The X Ray Diffraction spectra of TiN coatings deposited at 5 % presents diffraction peaks of  $\alpha$ TiN (200) and Ti<sub>2</sub>N (111) at 40.8, 43.1, 44.7 and 46.7°, with a slight decrease in the lattice parameter ( $a_{\text{TiN}} = 0.4205$  nm).

Between 10 and 15 % of  $N_2$ , the Ti-N coatings, the diffraction spectra present (111), (200), (220) and (311) planes at  $36.85^\circ$ ,  $42.19^\circ$ ,  $61.88^\circ$  and  $74.01^\circ$  corresponding to the fcc-TiN phase. In parallel we can noticed the presence of (111), (200) and (220) planes at  $40.84^\circ$ ,  $43.01^\circ$  and  $78.80^\circ$  correspond to the tetragonal  $Ti_2N$  phase.

At 20 %  $N_2$ , the structure exhibits (111) plane growth tendency with a gradually decrease of the (200) diffraction peak. to Lu *et al.* [4], found that with the increase of N content, the deposition rate of the film decreases, resulting in an increase of the surface diffusion ability of the nitrogen and titanium and the orientation changes from (200) to (111) [3].

However, at 30 %  $N_2$ , the TiN coatings showed small diffraction peaks, which is in good agreement with those revealed in previous works [5, and 6].

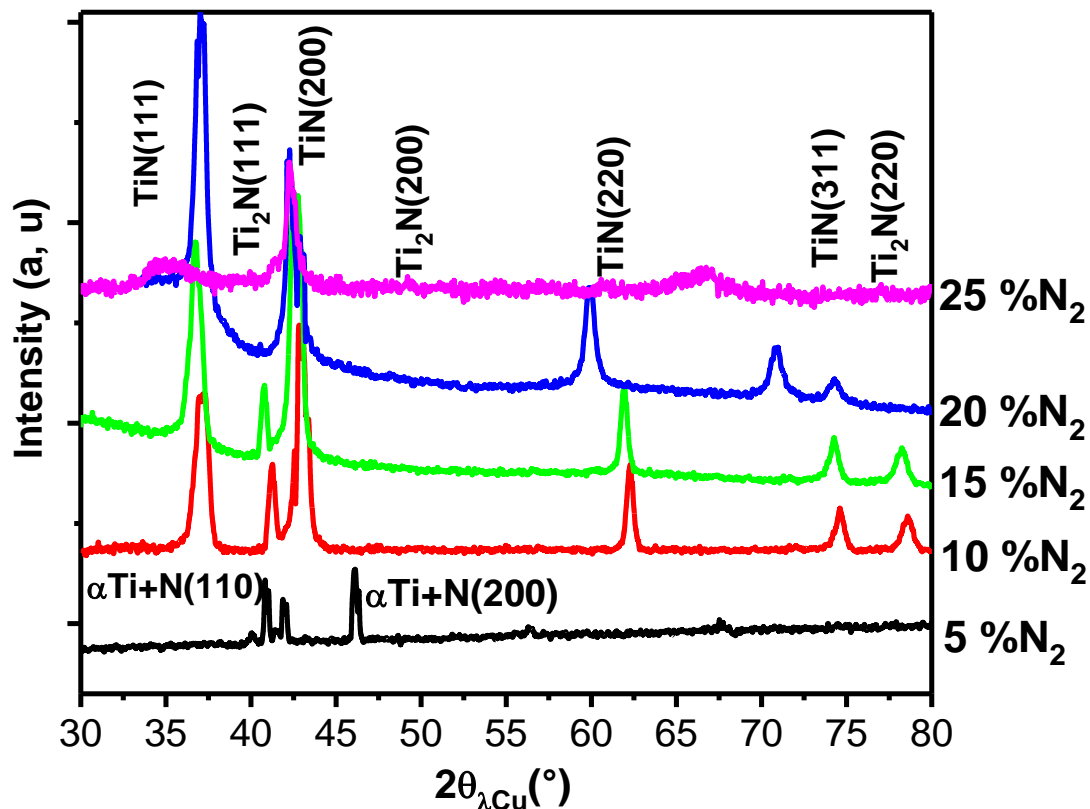


**Figure III. 1.** XRD spectra of the Ti-N coatings deposited at different nitrogen percentage.

In our work, the average crystallite size was determined by using Scherrer's equation [7]:

$$D = \frac{0.9\lambda}{\beta \cos \theta} \quad (\text{II. 1})$$

Where 0.9 is a dimensionless shape factor,  $\lambda$  is the X-ray wavelength ( $\lambda_{\text{Cu}} = 0.154 \text{ nm}$ ),  $\beta$  (in rad) is the line broadening at half the maximum intensity (full width half maximum) and  $\theta$  is the Bragg's angle of (111) TiN plane.

It has been revealed that the intensity of the predominant (111) plane increased with increasing nitrogen content. The lattice constant is also slightly increases when the N atoms can inserted in the interstitial positions of TiN lattice [8-9]. However, the crystallite size decreased from 80 down to 64 nm when the quantity of nitrogen increased from 14 to 48 at.%, (as listed in Table III. 2), which is in agreement with the results reported by Wan et *al*, for the sputtering chromium nitrides films [3].

### III. 3.3. Morphology

Figure III. 2 shows the SEM cross section and surface morphology of the TiN coatings deposited between 10 and 20 % of Nitrogen.

SEM images of the films deposited at different Nitrogen percentage show a significant decrease in the thickness are listed in Table III. 2. At 10 % of N<sub>2</sub> (Fig. III. 2 a), the Ti-N film exhibited a rough and a columnar structure with a spherical form. This is due to the existence of the mixture of Ti<sub>2</sub>N and TiN phases [10].

At 20 %, we can see columnar structure with a smooth surface with a small grain size, which attributed to the dense surface (Fig. III. 2 b).

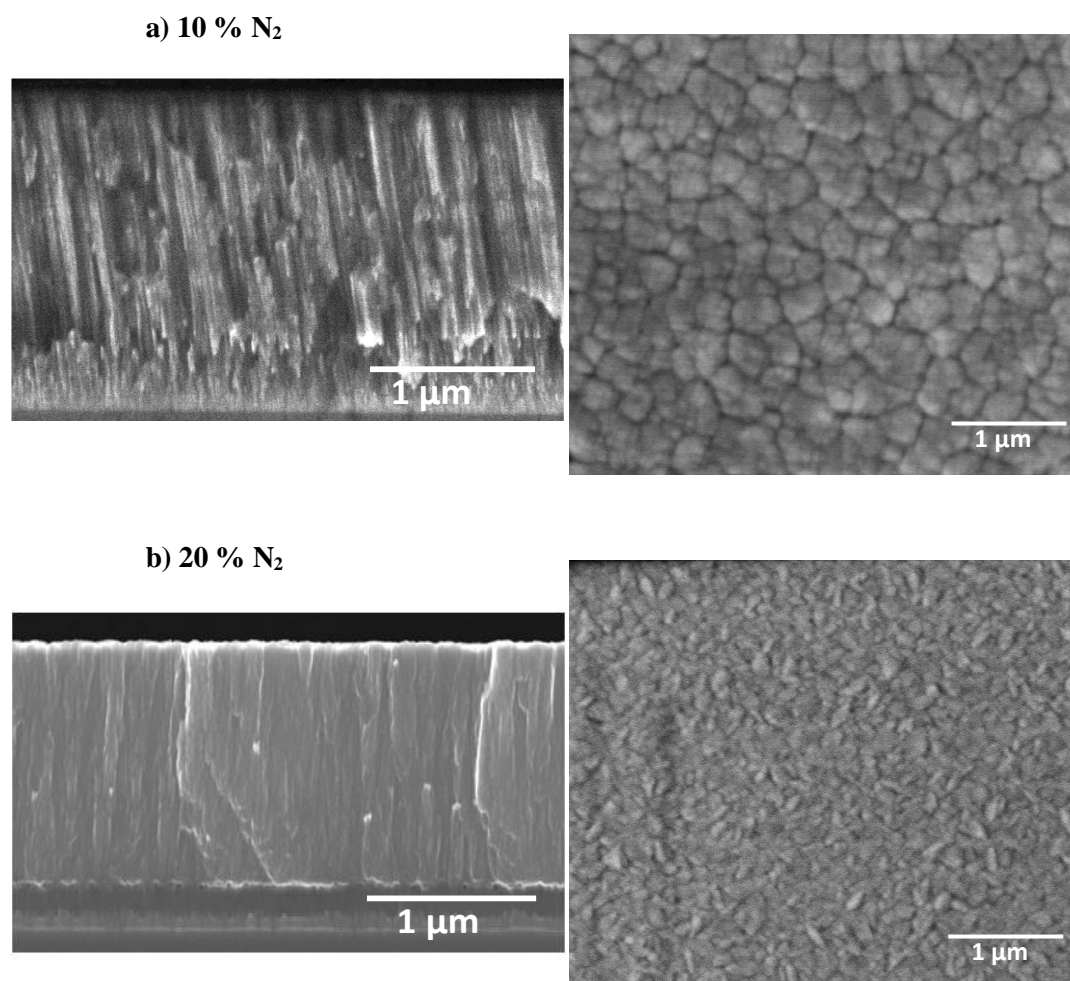


**Figure III. 2.** SEM cross section and surface images of the TiN coatings deposited at: a) 10 %N<sub>2</sub>, b) 20 %N<sub>2</sub>

### ***III. 3.4. Mechanical property***

Figure (III. 3) presents the hardness (H), elastic modulus (E) of TiN coatings as a function of the N<sub>2</sub> percentage. The evolution of elastic modulus presents a very similar curve as that obtained for hardness. At  $\leq 5$  % of N<sub>2</sub>, the hardness and elastic modulus are relatively low because of the low density of titanium nitride. With increasing the nitrogen amount, hardness and elastic modulus of TiN coatings gradually increased. The highest hardness (27.78 GPa) and elastic modulus (304.8 GPa) were obtained at 20 % of N<sub>2</sub>. This could be mainly attributed to the lower roughness and the fine grain size [11].

However, when the nitrogen flow rate increased above 25 %, the decrease in the hardness of TiN coatings was caused by the reduction of film thickness (from 1.26 to 0.97  $\mu\text{m}$ , Table III. 2) and the increase of the crystallite size (from 17 to 37 nm) [12, 13].

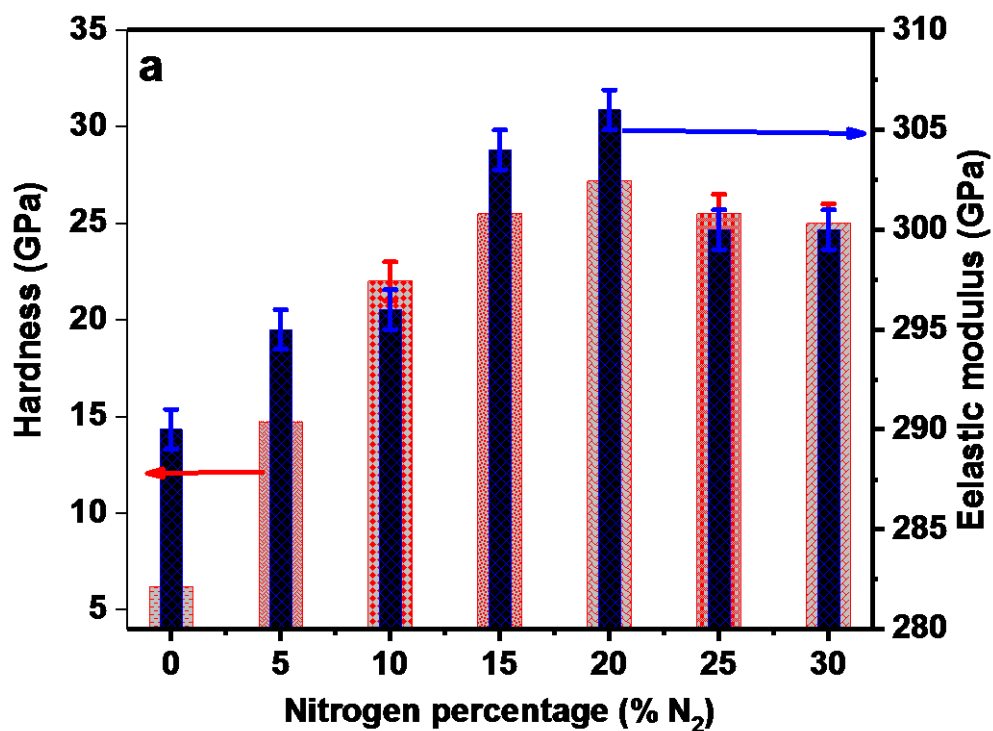


Figure III. 3. Hardness (H) and elastic modulus (E) of the TiN coatings at different N<sub>2</sub> percentage.

### III.4. Conclusion

Ti-N coating films were prepared using reactive magnetron sputtering technique with various nitrogen percentages.

X Ray Diffraction showed that the film phases changed from Ti to  $Ti_2N$  and TiN with increasing nitrogen percentage.

Increasing the nitrogen content in the TiN coatings conducts to increase the lattice parameter and a decrease the film thickness and crystallite size.

The increasing of the nitrogen content in TiN coatings film led the enhancement of surface density as mentioned by SEM images.

Nanoindentation measurements showed that hardness and elastic modulus of the TiN coatings exhibited an increase from (7.1 GPa, 195.2 GPa) to (27.78 GPa, 304.8 GPa) when nitrogen percentage was increased from 5 to 20 %, respectively.

---

**References**

- [11] M.F. Slim, A. Alhussein, E. Zgheib, M. François, Determination of single-crystal elasticity constants of the beta phase in a multiphase tungsten thin film using impulse excitation technique, X-ray diffraction and micro-mechanical modeling, *Acta Materialia* 175 (2019) 348-360.
- [12] Ponon, Nikhil K. "Effect of deposition conditions and post deposition anneal on reactively sputtered titanium nitride thin films." *Thin Solid Films* 578 (2015): 31-37.
- [13] X.S. Wan, S.S. Zhao, Y. Yang, J. Gong, C. Sun, Effects of nitrogen pressure and pulse bias voltage on the properties of Cr-N coatings deposited by arc ion plating, *Surf. Coat. Technol.* 204 (2010) 1800–1810.
- [14] L. Assaini, A. Alhussein, C. Nouveau, L. Ghelani, M. Zaabat, Influence of film thickness and Ar-N<sub>2</sub> plasma gas on the structure and performance of sputtered vanadium nitride coatings, *Surf. Coat. Technol.* 378 (2019) 124948.
- [15] D. Nath, F. Singh, R. Das, X-ray diffraction analysis by Williamson-Hall, Halder-Wagner and size-strain plot methods of CdSe nanoparticles- A comparative study, *Materials Chemistry and Physics* 239-122021 (2020) 1-9.
- [16] A. Kolitsch, X. Wang, D. Manova, W. Fukarek, W. Moeller, S. Oswald, Effects of titanium and aluminum incorporations on the structure of boron nitride thin films, *Diamond and Related Materials* 8(2–5) (1999) 386-390.
- [17] A. Obrosof, R. Gulyaev, M. Ratzke, A.A. Volinsky, S. Bolz, M. Naveed, S. Weiß, XPS and AFM investigations of Ti-Al-N coatings fabricated using DC magnetron sputtering at various nitrogen flow rates and deposition temperatures, *Metals* 7(52) (2017)1-10.
- [18] N. Arshi, J. Lu, B.H. Koo, C.G. Lee, F. Ahmed, Effect of nitrogen flow rate on the properties of TiN film deposited by beam evaporation technique, *Applied Surface Science* 258 (2012) 8498–8505.
- [19] J.E. Sundgren, Structure and properties of TiN coatings, *Thin Solid Films* 128(1-2) (1985) 21-44.
- [20] E. Lugscheider, K. Bobzin, Wettability of PVD compound materials by lubricants, *Surf. Coat. Technol.* 165 (2003) 51-57.
- [21] L. Aissani, A. Alhussein, A. Ayad, C. Nouveau, E. Zgheib, A. Belgroune, m. Zaabat R. Barille, Relationship between structure, surface topography and tribo-mechanical behavior of Ti-N thin films elaborated at different N<sub>2</sub> flow rates, *Thin Solid Films* 724 (2021) 138598.

- [22] D.G. Constantin, D. Munteanu, The influence of nitrogen content on the mechanical properties of TiN<sub>x</sub> thin films prepared by reactive magnetron sputtering, *Engineering Sciences* 5(54) (2012) 60-64.
- [23] L. Jun Hee, A. Joseph Nathanael, and Sun Ig Hong. "Effect of nitrogen flow rate on the structure and properties of TiN thin films deposited onto  $\beta$ -type Ti-15Mo-3Nb-3Al-0.2 Si alloy substrates by reactive magnetron sputtering." *Advanced Materials Research*. Vol. 557. Trans Tech Publications Ltd, (2012).

General conclusion

### *General conclusion*

Titanium nitride (TiN) coatings have a wide range of applications due to their practical features like excellent hardness, excellent corrosion resistance, heat resistance, and superior wear resistance so on. Where it can be deposited by physical vapor deposition (PVD) evaporation, sputtering, ion plating, and chemical vapor deposition (CVD)

The purpose of this work is to study the structural and morphological properties of TiN films deposited by magnetron sputtering at different nitrogen percentages on Si (100) and XC100 substrates with a circular Ti (99.99 % purity) target.

Thin films were deposited by R.F magnetron sputtering. Magnetron sputtering coating is a vacuum coating method that falls under the category of physical vapor deposition (PVD); the latter is ensures the formation of a highly adhered film on substrates at low temperatures.

The description of the TiN system shows the effect of nitrogen concentration on the formed phases. The Ti-N film exhibited at 10 % of N<sub>2</sub> a rough and a columnar structure with a spherical form this is due to the existence of the mixture of Ti<sub>2</sub>N and TiN phases with a N/Ti ratio is around 0.28. At 20 %, we can see the columnar structure with a smooth surface with a small grain size, which attributed to the dense surface

Nanoindentation measurements showed that hardness and elastic modulus of the TiN coatings exhibited an increase from (7.1 GPa, 195.2 GPa) to (27.78 GPa, 304.8 GPa) when nitrogen percentage was increased from 5 to 20 %, respectively.

# Abstract

## Abstract

Transition-metal carbides and nitrides have attracted much attention for technological purposes. They are very hard, having good thermal conductivity, and good corrosion and wear resistances. Among them, titanium nitrides are very well-known materials widely applied as hard wear resistant protective coatings for cutting tools and other components. The addition of nitrogen to titanium enhances mechanical and tribological properties, and increases significantly the oxidation resistance which is due to the formation of a dense FCC-TiN phase.

In this work, we investigated the effect of nitrogen concentration on the structure and properties of Ti-N coatings deposited by magnetron sputtering. The structural and morphological properties of TiN films were described, and followed by a detailed investigation on the mechanical properties of Ti-N coatings. By varying the nitrogen percentage, the structure and the hardness of Ti-N films were evaluated in a wide range. With rising N<sub>2</sub> injected in the deposition chamber, the structure changed from Ti<sub>2</sub>N at 10 % N<sub>2</sub> to a mixture of Ti<sub>2</sub>N and TiN at 20 %N<sub>2</sub>. The hardness of the films first augmented with increasing the nitrogen percentage and take a maximum value was 32 GPa for the films deposited under 20 %N<sub>2</sub> then decreased.

**Keywords:** *Ti-N thin films; Magnetron sputtering; microstructure, hardness.*

---

### *Résumé*

Les carbures et nitrures de métaux de transition ont beaucoup d'attraction dans plusieurs objectifs technologiques. Ils sont très durs, ont une bonne conductivité thermique et une bonne résistance à la corrosion et à l'usure. Parmi eux, les nitrures de titane sont des matériaux largement connus et ont des applications importantes comme revêtements protecteurs résistants à l'usure pour les outils de coupe et autres composants. L'ajout d'azote au titane améliore les propriétés mécaniques et tribologiques, et augmente considérablement la résistance à l'oxydation résultant de la formation d'une phase dense FCC-TiN.

Dans ce travail, nous avons étudié l'effet de la concentration d'azote sur la structure et les propriétés des revêtements de TiN déposés par pulvérisation magnétron. Les propriétés structurales et morphologiques des films de TiN ont été décrites et suivies d'une étude détaillée des propriétés mécaniques des revêtements de Ti-N. En modifiant le pourcentage d'azote, la structure et la dureté des couches de Ti-N ont été largement évaluées. Avec l'augmentation du N<sub>2</sub> injecté dans la chambre de dépôt, la structure est passée de Ti<sub>2</sub>N à 10 % N<sub>2</sub> à un mélange de Ti<sub>2</sub>N et TiN à 20 % N<sub>2</sub>. La dureté des couches augmente d'abord avec l'augmentation du pourcentage d'azote et prend une valeur maximale de 32 GPa pour les couches déposés sous 20 % de N<sub>2</sub> puis elle diminue.

**Les mots clés :** couches minces Ti-N ; Pulvérisation magnétron; microstructure, dureté.

---

## الملخص

كربيدات والنتريدات المعادن الانتقالية جذبت الكثير من الاهتمام للأغراض التكنولوجية. ، لديها موصلية حرارية جيدة ، ومقاومة جيدة للتآكل كما أنها صلبة للغاية. من بينها ، نيتريد التيتانيوم عبارة عن مواد معروفة جيداً يتم تطبيقها على نطاق واسع كطلاءات واقية مقاومة للاهتراء لأدوات القطع والمكونات الأخرى. تعزز إضافة النيتروجين إلى التيتانيوم الخواص الميكانيكية والتريبولوجية ، وتزيد بشكل كبير من مقاومة الأكسدة التي تنتج عن تكوين طور كثيف FCC-TiN.

في هذا العمل ، درسنا تأثير تركيز النيتروجين على بنية وخصائص طبقات Ti-N المترسبة بواسطة رش المغنطرون. حيث تم وصف الخصائص الهيكلية والمورفولوجية لأغشية TiN ، وتبعها تحقيق مفصل حول الخواص الميكانيكية لطلاءات Ti-N. من خلال تغيير نسبة النيتروجين ، تم تقييم هيكل وصلابة أفلام Ti-N في نطاق واسع. مع ارتفاع N<sub>2</sub> المحقون في غرفة الترسيب، تغير الهيكل من Ti<sub>2</sub>N عند 10% N<sub>2</sub> إلى خليط من TiN و Ti<sub>2</sub>N عند 20%. ازدادت صلابة الأغشية أولاً مع زيادة نسبة النيتروجين وأخذت قيمة قصوى كانت 32 جيجا باسكال للأغشية المودعة تحت 20% N<sub>2</sub> ثم انخفضت.

الكلمات المفتاحية : أغشية Ti-N الرقيقة ؛ المغنطرون الاخرق؛ البنية المجهرية والصلابة.